Lung imaging methods: indications, strengths and limitations

Dávid László Tárnoki[1,2], Kinga Karlinger[1], Carole A. Ridge[3,4], Fanni Júlia Kiss[1], Tamás Györke[1], Elzbieta Magdalena Grabczak[5] and Ádám Domonkos Tárnoki[1,2]

[1]Medical Imaging Centre, Semmelweis University, Budapest, Hungary. [2]Oncologic Imaging and Invasive Diagnostic Centre and the National Tumor Biology Laboratory, National Institute of Oncology, Budapest, Hungary. [3]Department of Radiology, Royal Brompton and Harefield Hospitals, London, UK. [4]National Heart and Lung Institute, Imperial College London, London, UK. [5]Department of Internal Medicine, Pulmonary Diseases and Allergy, Medical University of Warsaw, Warsaw, Poland.

Corresponding author: Dávid László Tárnoki (tarnoki4@gmail.com)

Shareable abstract (@ERSpublications)
Imaging methods are fundamental tools to detect and diagnose lung diseases, monitor their treatment and detect possible complications. Each modality has its strong and weak points, which we should be familiar with to properly choose the methods. https://bit.ly/3XRnnAC

Cite this article as: Tárnoki DL, Karlinger K, Ridge CA, *et al*. Lung imaging methods: indications, strengths and limitations. *Breathe* 2024; 20: 230127 [DOI: 10.1183/20734735.0127-2023].

Received: 15 Jan 2024
Accepted: 24 June 2024

Abstract

Imaging methods are fundamental tools to detect and diagnose lung diseases, monitor their treatment and detect possible complications. Each modality, starting from classical chest radiographs and computed tomography, as well as the ever more popular and easily available thoracic ultrasound, magnetic resonance imaging and nuclear medicine methods, and new techniques such as photon counting computed tomography, radiomics and application of artificial intelligence, has its strong and weak points, which we should be familiar with to properly choose between the methods and interpret their results. In this review, we present the indications, strengths and main limitations of methods for chest imaging.

Educational aims

- To understand the indications, strengths and limitations of diagnostic imaging methods and nuclear medicine methods in respiratory medicine.
- To learn about the role of interventional radiology in respiratory medicine.

Introduction

Lung imaging studies are vital in the assessment and follow-up of lung diseases. In this review, we will cover the basics and the roles of imaging techniques in respiratory diseases, mainly focusing on radiography, lung ultrasound and computed tomography (CT). Novel applications of existing imaging techniques, such as hyperpolarised gas magnetic resonance imaging (MRI) and positron emission tomography (PET), show promise in combining structural and functional information [1]. The significant role of image-guided lung interventions will also be delineated.

Chest radiography and fluoroscopy

Wilhelm Conrad Röntgen accidentally discovered X-rays in 1895 during his experiments with a cathode ray tube. Despite the many imaging techniques created since that time, chest radiography (CXR), in the majority of cases, is still the first imaging modality performed in cases with symptoms in the lungs and airways, having a firm position in the algorithm for examining patients as well as in follow-up after interventional procedures on lungs, airways or vessels.

The main advantages of CXR include its wide availability, low cost and radiation, and rapid results. The examination may be performed either in a radiology unit or at the bedside. The disadvantages of CXR are its limited specificity and sensitivity in many cases, as well as the radiation dose, which may especially be a disadvantage in children and pregnant women (table 1).

Chest fluoroscopy is a diagnostic imaging procedure that uses a continuous X-ray beam to create real-time images of the chest if the diagnosis is questionable on CXR [4]. Its main disadvantages are additional

TABLE 1 Characteristics, indications and limitations of various lung imaging modalities

	CXR	Ultrasound	CT	PET	MRI
Safety (radiation)	Dose 0.1 mSv	No radiation	ULDCT 0.2–0.3 mSv, LDCT 0.5–1.5 mSv, PCCT 0.3–1 mSv, conventional CT ~6.1 (2–20) mSv	PET 7–8 mSv, total dose for PET/CT 16–26 mSv	No radiation
Costs	Low	Low	High	High	High
Advantages	Low cost, low radiation exposure, high availability, portable, rapid result	Low cost, no radiation, high availability, portable, sensitive (*e.g.* better than CXR for pneumonia or pneumothorax in supine position and better than CT in detection of pleural septations or malignant infiltration of chest wall), helpful in emergency situations, can be used at point of care	Higher sensitivity than CXR and in many cases than ultrasound, allows for real-time CT-guided procedures	Analyses based on cell metabolism, detection of disease at early stage, differentiation between inflammation and malignancy, better assessment of treatment outcome	Assessment of mediastinum, vessels or chest involvement; no ionising radiation
Contra-indications	None (considered safe in pregnancy below 50 mGy)	No contraindications	Impaired renal function and thyroid function, allergy to contrast agent, pregnancy (+/–), radiation (especially young people or breast exposure), dyspnoea enabling supine position, morbid obesity	Relative: pregnancy, morbid obesity, claustrophobia	Allergy to contrast agent, metal implants, pacemakers and other electronic devices (some allowed), severe renal failure (gadolinium)
Limitations	Low sensitivity, low specificity	Only peripheral lesions attaching the pleura are visible	Performance only in CT room	Lesions <8 mm, time of radioactive decay, risk of false positive results after meal or in diabetic patients	Low availability, long study acquisition time
Application in selected situations					
Asthma	+/–	–	+	–	+/–
COPD	+	–	+	–	+/–
Pneumonia	+	+	+	+/–	+/–
Lung carcinoma	+	+/–	+	+	+
ILD plus fibrosis	+	+/–	+	+/–	+/–
ILD plus cystic lung diseases	+	+/–	+	–	–
Pleural diseases	+	+	+	+	+
Pulmonary embolism	+/–	+/–	+	+ (*V′*/*Q′* PET/CT)	+
Pulmonary hypertension	+	+/–	+	–	+/–
Assessment of chest drain or central line position	+	–	+	–	–
Diagnostics or interventional procedure	+	+	+	–	–

CXR: chest radiography; CT: computed tomography; PET: positron emission tomography; MRI: magnetic resonance imaging; ULDCT: ultra-low-dose CT; LDCT: low-dose CT; PCCT: photon counting CT; ILD: interstitial lung disease; +: applicable; –: not applicable; +/–: not a routine indication for this imaging modality, but some characteristic abnormalities can be detected in some cases; *V′*/*Q′*: ventilation/perfusion. Data from [2, 3].

radiation exposure, poor spatial resolution and subjective evaluation. During fluoroscopy, deviation of the diaphragm and the pendulum movement of the mediastinum during inhalation and exhalation can be observed. For example, in Holzknecht–Jacobsen syndrome, an obstructed bronchus causes paradoxical movement of the mediastinum towards the lung with the obstructed bronchus during inhalation [5].

Contrast-enhanced radiographs can also be performed, such as a contrast-enhanced barium enema to examine a hiatal hernia or oesophageal perforation.

CXR allows assessment of the lungs, pleura, mediastinum, big vessels, size of the heart, bones and upper abdomen (figure 1a). A detailed description of abnormalities that can be seen by CXR is beyond the scope of this article. In general, air appears as black or dark, fat is shown as dark grey, fluids and soft tissue show a light grey appearance, and bones are not translucent (white). Sometimes a lung opacity may not originate from the lungs, but from the chest wall (*e.g.* fibrous pleural tumour), skin (nipple or naevus) or may be localised outside the patient. A radiopaque tag can be used to mark abnormal findings on the skin to clarify the source of the CXR findings.

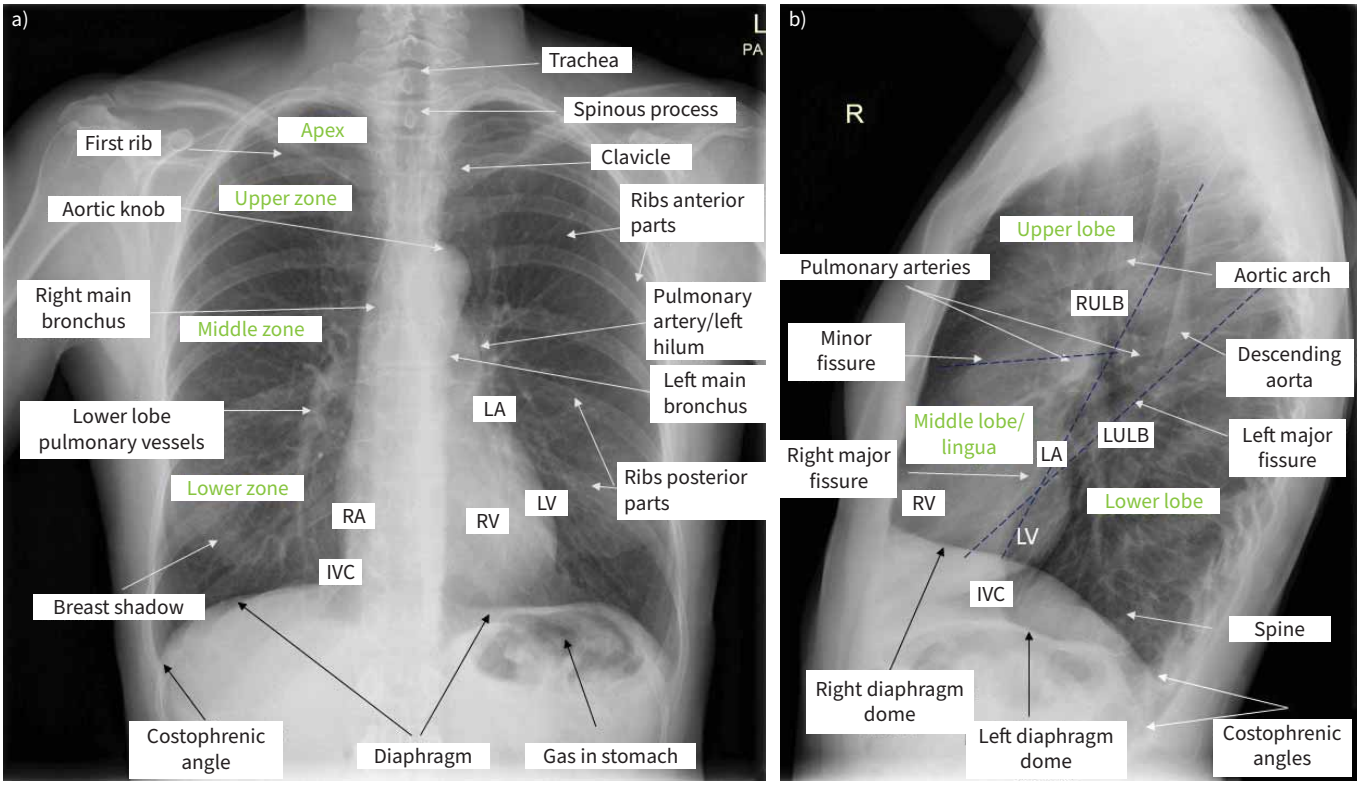

FIGURE 1 Normal chest radiography in upright position. a) Posterior–anterior view. Visible structures and lung zones are presented. Breast tissue can increase attenuation of the X-ray beam in the lower lung zones. The heart, diaphragm and liver are in contact; no line separating them is visible. Assessment should include: chest wall bones (if fracture or lesions present); heart and vessels (cardiac silhouette should occupy less than half of the transverse diameter of the thoracic cavity, mediastinal width ⩽8 cm, aortic knob well defined); diaphragm and upper abdomen (right hemidiaphragm is slightly higher than the left one, the costophrenic angles should not be blunted, no air beneath diaphragms); and lungs (lung fields clear (without opacities or other lesions), lung markings visible to the periphery (may be less prominent in apices), assessment for pneumothorax and presence of pleural fluid; while assessing the lungs, each lung region should be compared on both sides). The proper acquisition of the image incudes: exposure (intervertebral spaces in the thoracic part and vessels through heart and diaphragm shadow should be visible; overexposed radiographs are black, and underexposed radiographs are nearly white); symmetry (distance between sternal endings of clavicles and spinous processes should be similar; asymmetric images cause enlargement of mediastinal structures); depth of inspiration (the diaphragm should be below the inferior part of the 10th rib; poor inspiration may simulate pulmonary oedema and may hide small nodules); and elimination of breathing artefacts (if patients hold their breath during the examination, the shape of the heart, diaphragm and vessels will be sharp). b) Lateral view. Typical is lucent (dark) retrocardiac and retrosternal space and posterior diaphragmatic recess. Progressive lucency (darkening) of the thoracic spine as it approaches the diaphragm is visible and called spine sign. If not present, may suggest opacity (infiltrate or pleural effusion). RA: right atrium; RV: right ventricle; LA: left atrium; LV: left ventricle; IVC: inferior vena cava; RULB: right upper lobe bronchus; LULB: left upper lobe bronchus.

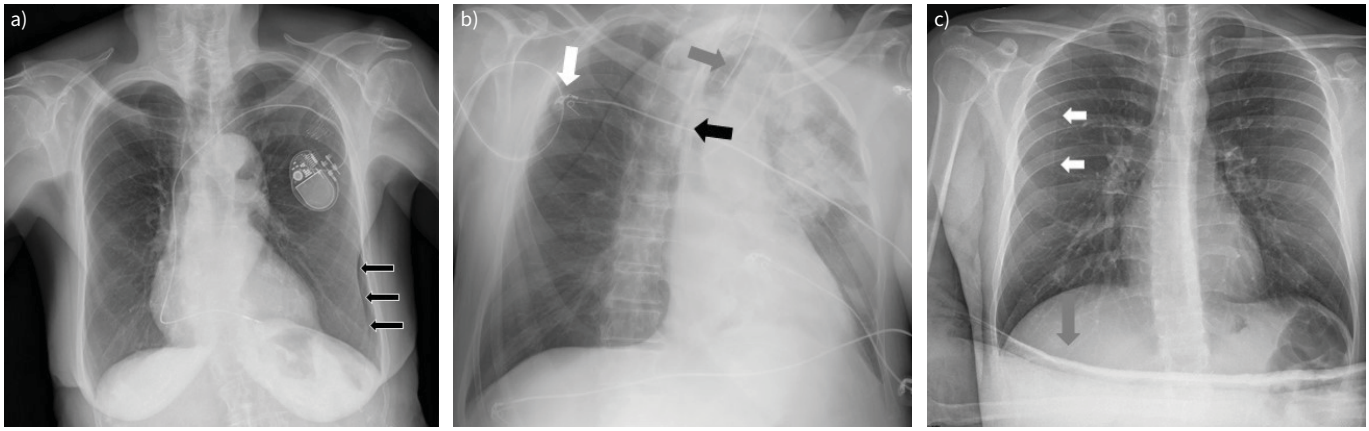

FIGURE 2 Limitations in chest radiography. a) Arrows: skin folds, which may mimic pneumothorax. b) External devices. Patient in intensive care unit, supine position posterior–anterior view. White arrow: ECG monitoring cables; grey arrow: endotracheal tube; black arrow: catheter in superior vena cava. Rotation of the image causes a shift of mediastinum to the left side. c) White arrows: border of scapula, which may mimic pneumothorax; grey arrow: patient's hand.

Conventional bidirectional CXR includes a posterior–anterior (PA) view (the X-ray beam traverses the patient from posterior to anterior) and lateral projections with the patient in a standing position, with the scapula pulled laterally for better visualisation. CXR is performed with 120–130 kVp and approximately 5 mAs with a focus–film distance of 2 m, in deep inspiration. The lateral view (labelled with the side closest to the cassette) is not routinely performed but may be important as it provides data about the localisation of abnormalities, and demonstrates retrosternal and retrocardiac space and posterior costophrenic recesses (figure 1b).

In patients in a supine position, only anterior–posterior (AP) CXR may be performed, which is frequently connected with artefacts (rotation, poor inspiration, skin folds, or shadows of concomitant devices) (figure 2). When the examination is performed with a portable device at the bedside, the distances between X-ray tube and patient and detector are smaller. Moreover, both supine position and AP technique result in enlargement of the cardiac silhouette and mediastinal structures, elevation of the diaphragm, compression of lower lobes, decreased diameter of the lungs, as well as signs of cardiac congestion (due to vascular alveolar fluid redistribution in the upper lobes). They also alter the appearance of pleural effusions and pneumothorax [2].

Rarely, CXR is performed in the lateral decubitus position, which used to be considered for the detection of small amounts of pleural effusion (5 mL), small pneumothorax (15 mL of air), air trapping in case of a foreign body or pneumomediastinum, or differentiation of parenchymal consolidation from pleural effusion [6, 7].

Accurate assessment of the CXR depends on correct performance. CXR may falsely simulate pathology or obscure important abnormalities (figure 2). Moreover, the quality of the image depends on the focused radiation, the quality of the detector system, the distance between the object and the image plane, and the patient's body shape (*e.g.* obese patients produce more scattered radiation) (figure 3a).

Digital chest tomosynthesis, by the single rotation of the X-ray tube around the patient, produces an arbitrary number of section images of the chest at lower cost and radiation dose than CT, improving the detection of subtle lung disease, such as nodules, over conventional CXR.

The use of chest fluoroscopy, contrast-enhanced radiographs and artificial intelligence in CXR assessment is beyond the scope of this article. Post-processing techniques can be used to improve the image quality of the digital CXR images, such as windowing, magnification and grey-scale inversion [8].

Thoracic CT

Lungs and pleura

CT is the best imaging method for the chest. It is readily available, reliable and quick, with excellent spatial resolution. Photon counting computed tomography (PCCT) provides two and even three (volumetric)

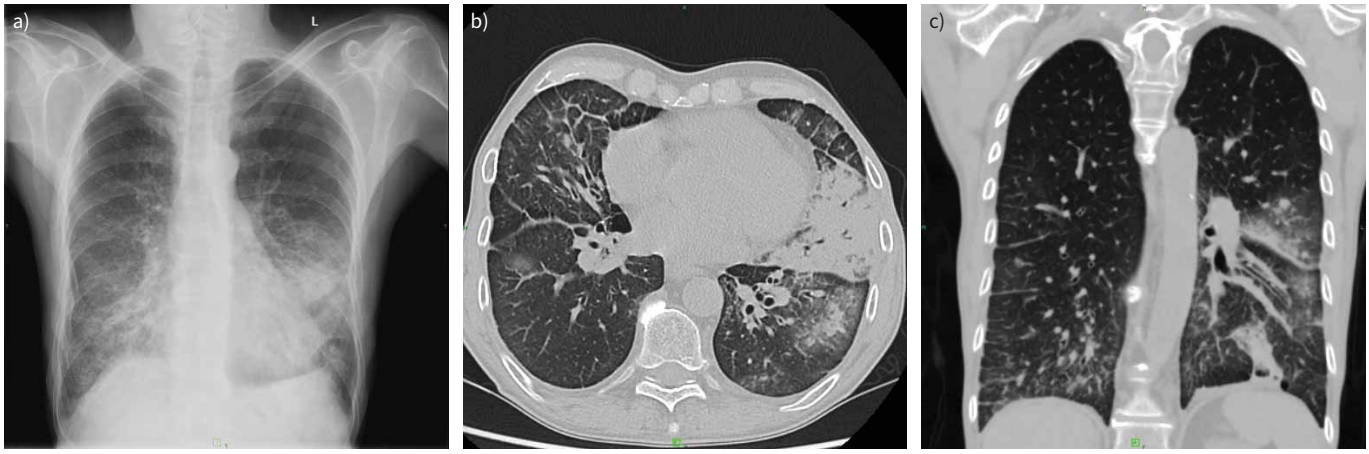

FIGURE 3 59-year-old male patient with a history of sublingual cancer with a sudden onset of dyspnoea. a) Chest radiograph demonstrated infiltrates and ground-glass opacity in basal distribution. Coronavirus disease 2019 (COVID-19) was suspected; therefore, a computed tomography (CT) scan was requested. b) Axial and c) coronal CT images depicted patchy nodular consolidations in the right lobe and in the left lung, mainly in peribronchial localisation. Extensive ground-glass regions could be observed around these areas. In the ventrobasal part of the left segment S3, a triangular consolidation area with a black bronchus sign was also detected, and a similar consolidation in the left S10. Bilateral few band-like lesions and pleural effusion were also visible. The depicted pulmonary abnormalities primarily indicated bronchopneumonia; COVID-19 pneumonia was considered less likely (CO-RADS category 2 (COVID-19 Reporting and Data System)).

dimensions through reconstruction. ECG triggering can be useful for CT angiography and calcium scoring of the coronary vessels.

Clinical questions that may be addressed by thoracic CT can relate to the following lung disorders: congenital lung disease, pneumonia, interstitial lung disease, bronchiectasis, tumours (benign or malignant), diseases of the pleura (inflammatory diseases, primary/secondary tumours, or fluid producing diseases), diseases involving the mediastinum, and chest trauma.

The strengths of CT include that it is noninvasive, quick, painless and widely available. Imaging can be performed in a way that is geometrically correct (*e.g.* for irradiation therapy, by cone beam/flat panel CT). Additionally, all the X-ray attenuation values caused by several types of tissues are imaged together and can be evaluated separately but at the same time (lung tissue, soft tissues, cartilage, bone and blood vessels; the latter can even be enhanced by intravenous iodinated contrast material). Another advantage is that procedures such as lung biopsy and pleural cavity aspiration can be performed with guidance of real-time CT, instead of needing more invasive operative procedures.

A weakness of CT is that the potential for ionising radiation creates a need for low-dose imaging, when possible. Thus, the soft-tissue contrast of MRI may be a useful alternative to CT. Further limitations in using CT scans are that they may not be suitable in the case of morbid obesity, or in patients who cannot lie still or flat. CT imaging during pregnancy also requires a risk–benefit analysis.

Pulmonary anatomy

Pulmonary anatomy may be studied through thoracic CT. The architecture of the lungs consists of central and peripheral (peribronchovascular) interstitium, which is continuous with centrilobular interstitium (inside the secondary pulmonary lobule). The secondary pulmonary lobule is organised from bronchovascular bands and secondary lobuli (anatomical and functional units of the lungs). Bronchi and arteries run together from the hila to the periphery, dividing parallel in a dichotomous way, then enter the secondary lobules giving the hexagonal/polyhedral form. Veins run peripherally in the walls (interstitium) of the secondary lobule together with the main lymphatic channels. 400–500 alveoli constitute one acinus (7 mm diameter), and three to seven acini constitute one secondary lobule (1.5–2 cm diameter). Between alveoli are the pores of Kohn, through which tumour or infections may spread. Gas exchange occurs in the alveoli *via* the terminal bronchiole (the end of the airway). The interstitium consists of three compartments: bronchovascular (axial), parenchymal (acinar) and subpleural. Lymphatic drainage takes place centrally along the bronchovascular bundles and peripherally in the interlobular septa, along the pleural lining. There is smaller lymphatic drainage centrally.

Some features and processes occurring in the secondary lobuli can be seen correctly only by high-resolution computed tomography (HRCT). For example, in the interstitium (perilymphatic area), cellular infiltration due to tumour spreading (even axial) dilates the secondary lymphatic routes. In addition, widened interstitial septa can be caused by mitral stenosis in case of cardiac congestion (stasis), which is visible as Kerley lines A and B on CXR. Depending on the cause, widening of the interstitial septa can be reversible.

Arterioles of 0.2 mm diameter can be shown by HRCT, but not their concomitant bronchi (because they have tiny walls). Interstitial inflammation (pneumonitis), which can later become interstitial (chronic) lung diseases, and idiopathic interstitial pneumonitis, can also be observed through HRCT. Furthermore, in the centrilobular lung, hypersensitivity pneumonitis (HP), respiratory bronchiolitis and centrilobular emphysema can be seen. The centrilobular lung is the central part of secondary lobuli, and these defects can be caused from the outside environment or *via* the circulation, *via* an artery together with a bronchus that enters here.

CT patterns indicating disease

Typical patterns of the lungs seen on thoracic CT characterise several diseases. These will be discussed in the following sections.

Ground-glass opacities

Ground-glass opacities (GGOs) indicate alveoli that are stuffed with oedematous liquid, pus, blood or invading cells (inflammatory or tumorous). The origin can be interstitial (fibrosis) thickening of the alveolar walls, but this depends on the underlying disease: inflammatory, early fibrosis, haemorrhage or haemodynamic disease (cardiogenic or capillary). GGOs can be acute (due to oedema (cardiac or acute respiratory distress syndrome (ARDS)), haemorrhage (granulomatosis with polyangiitis) or pneumonia (mostly viral, but also due to *Mycoplasma*, acute eosinophilic or *Pneumocystis jirovecii* pneumonia (PJP)) (figure 3)) or chronic (due to HP, cryptogenic organising pneumonia (COP), alveolar proteinosis, lung fibroses (usual interstitial pneumonia (UIP) or nonspecific interstitial pneumonia (NSIP)) or lepidic-predominant adenocarcinoma).

Localisation of the GGOs will give further indications of the disease: upper zone GGOs may be due to respiratory bronchiolitis or PJP, lower zone GGOs due to UIP or NSIP, and centrilobular GGOs due to HP or respiratory bronchiolitis. GGO formation is an active process, and before fibrosis it can be healed by treatment. The investigation/follow-up method should be HRCT.

Consolidation

In a consolidation, attenuation of the lung (a part of it) is high, and the air in the alveoli and (smaller) air ducts is replaced by cellular elements/fibrosis (figure 4a). Mild forms are characterised by the dark bronchus sign (figure 3). Total attenuation causes the black bronchus sign, which can even be seen by CXR (for example in infant respiratory distress syndrome). The chronic form may indicate COP. The investigation/follow-up method should be HRCT.

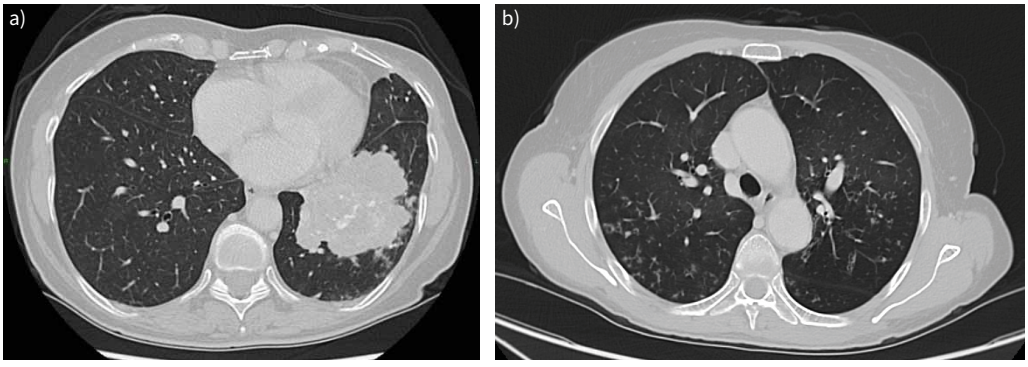

FIGURE 4 Axial computed tomography. a) Consolidation in the left lower lung lobe. Histology confirmed lung adenocarcinoma. b) Tree-in-bud phenomenon, mucus plugs and bronchial wall thickening, corresponding to bronchiolitis.

Tree-in-bud phenomenon

The tree-in-bud phenomenon affects the centrilobular bronchioli, which are dilated, with thickened walls and impacted lumens; there is also concomitant inflammation. It gives a V- or Y-like pattern (figure 4b). The cause of impaction can be mucus, pus or fluid. Additional indirect signs are air trapping at exhalation and/or subsegmental consolidation. This pattern was first described in tuberculosis but later revealed in other diseases: infectious (bacterial, viral, parasitic or mycotic), tumorous, immunological or congenital, or those due to inhalation of irritative materials (and those with unknown cause). The investigation method should be HRCT.

Crazy paving

The "crazy paving" pattern is a combination of GGO and septal thickening. It was first described in alveolar proteinosis but there are several other diseases with this type of pattern: sarcoidosis, NSIP, COP, infections (such as PJP, viral, mycoplasmic and other bacterial infections), neoplasms (such as lepidic-predominant adenocarcinoma), haemorrhage, oedema (cardiac), ARDS and acute interstitial pneumonia. The investigation method should be HRCT.

Mosaic attenuation

Mosaic attenuation patterns are patterns of mixed attenuations (high and low together or near each other), causing patchy features [9–11]. HRCT series should be performed during inspiration and even expiration, because underlying problems are various: normal and air trapping, normal and infiltrative, oligemic (thromboembolic) and hyperperfused are variously near each other. The investigation method should be HRCT.

Honeycombing

The "honeycombing" pattern features small cystic-like rows near each other, beginning peripheral-subpleural, at the base of the lungs, and continuing upwards to the pulmonary apex. This pattern is independent of causing factor, such as autoimmune diseases or chemotherapeutics. Idiopathic pulmonary fibrosis with UIP is the most characteristic picture. GGO precedes honeycombing, showing where the inflammatory fibrosing process is active. The investigation/follow-up method should be HRCT.

Low attenuation patterns

Low attenuation patterns are caused by increased air content at the level of the secondary lobule, due to emphysema, cystic alterations in the lung (such as lymphangioleiomyomatosis, lymphocytic interstitial pneumonia or Langerhans cell histiocytosis), and even honeycombing and bronchial dilation (bronchiectasis). The investigation method should be HRCT.

Emphysema

Emphysema in the secondary lobuli can be centrilobular, panlobular or paraseptal (distal acinar). Centrilobular emphysema is mainly seen in (excessive) smokers, with dilating/destruction of bronchioli, predominantly in the upper lobe. In panlobular emphysema, the entire secondary lobulus is involved. Alveolar ducts and alveoli are dilated in a destructive way, and respiratory ducts can even be dilated. Panlobular emphysema is found predominantly in the upper lobe. Most patients have a lack of α_1-antitrypsin, and smokers also tend to develop it. Paraseptal emphysema is found near the pleura and interlobular septa, on the periphery of secondary lobuli. It can cause bullae, even huge ones (creating pneumothorax, especially in young males). Contributing factors are smoking, ageing and male sex. In interstitial pulmonary processes, paraseptal emphysema occurs even more often. The investigation method for all emphysema should be CT/HRCT.

Bronchial dilation

In normal cases, bronchi and their concomitant arteries have the same diameter (HRCT shows this 1:1 ratio). Bronchiectasis/bronchus dilation widens the bronchial lumen(s); when this is extreme, the "signet ring sign" is seen on HRCT (and can even be detected by artificial intelligence). A consequence of pulmonary fibroses is also dilation of bronchi, by a traction mechanism. It is possible to follow these out to the periphery. The investigation method should be HRCT.

Heart and vessels

Cardiac computed tomography angiography (CCTA) has undergone considerable advances in recent years, resulting in more accurate and earlier diagnosis of aortic and coronary artery disease (CAD). These advances include the increased number of X-ray tubes and detectors and improved detector technology in CT scanners, leading to improved spatial and temporal resolution and lower radiation dose. The most recent development, PCCT, will further improve coronary imaging by minimising the effect of calcified

plaque on image quality and offering further CT radiation dose reduction [12]. This section of our review will summarise clinical image acquisition, technology and applications of coronary CT.

CCTA involves injecting a timed volume of contrast medium into a peripheral vein to delineate the coronary arteries and great vessels, during a CT scan. The patient lies supine, and images are acquired during held shallow inspiration while chest electrodes provide ECG synchronisation with the CT tube. ECG gating ensures images are acquired only at specific intervals in the cardiac cycle, typically diastole, thus reducing motion artefact. Computer algorithms reconstruct these images into thin section images that can then be converted into multiplanar representations, which demonstrate coronary stenosis, plaque burden and anatomy. In the case of coronary CT, pharmacological vasodilation and rate control are often required [13]. Glyceryl trinitrate and a beta blocker are given to maintain a heart rate of 60–70 beats·min^{-1}; the degree of rate control is dependent on the generation of CT scanner [14].

A CT tube, generating an X-ray beam, creates CCTA images by being mounted on a moving cylinder called a gantry. Within the CT tube, electrons are accelerated across a potential difference, striking a metal target in the tube, and then passing through a collimator to generate a focused beam of X-rays. The rotating gantry then turns around the patient in a craniocaudal direction, emitting X-ray beams from multiple angles. These X-rays are absorbed in varying degrees of magnitude, a process known as attenuation, and then detected on the opposite side. The attenuation data are reconstructed into thin section images. CT detectors are typically composed of materials that convert X-ray energy into electrical signals. The amount of signal generated corresponds to the attenuation value of each part of the patient, with a unit known as the Hounsfield unit.

The limitations of CT include the prohibitive effect of densely calcified plaque, often seen in the elderly population, which can cause overestimation of stenosis. Cardiac CT is also limited as a screening tool due to its inherent radiation dose and use of pharmacological rate control and iodinated contrast.

PCCT detects and counts individual X-ray photons. Only X-ray data above a certain energy threshold are collected, omitting low energy noise. This results in a higher contrast to noise ratio. Detectors are separated by anti-scatter blades, and this can vastly improve the spatial resolution of CT as well. There is less signal loss as a result and, specific to coronary CT, this minimises streak artefact related to calcified plaque. PCCT may, in the future, address many of the perceived limitations associated with cardiac CT [15].

CCTA is the preferred test in patients with a low clinical likelihood of CAD, no previous diagnosis of CAD, and characteristics associated with a high likelihood of good image quality. The UK National Institute for Health and Care Excellence (NICE) guidelines for the investigation of patients with chest pain recommend the use of CCTA as a first-line investigation in patients with new-onset stable chest pain [16]. CT is also now extensively used prior to structural heart interventions, *e.g.* for pre-procedural planning in advance of transcatheter aortic and mitral valve replacement, atrial appendage closure and the treatment of septal defects. The advantages of this approach include rapid image acquisition, minimal motion artefact, and data that are easily reproducible across centres.

Pulmonary arterial CT angiography is sensitive for pulmonary thrombosis and can also detect pulmonary arteriovenous malformations or aneurysm. It is the test of choice in the assessment of suspected pulmonary embolism. ECG gating is not typically required for this technique. The timed volume of contrast medium is injected when contrast is opacifying the pulmonary arterial tree at held shallow inspiration, to avoid excessive Valsalva effect, which could cause mixing of the unopacified blood pool from the inferior cava with injected contrast, usually administered through an upper limb vein.

Quantitative techniques can assist diagnosis and treatment decisions. Two examples include clot burden indices, such as the Qanadli index [17], and pulmonary iodine distribution quantification. Clot burden indices require the interpreter to count the amount and measure the size of thromboses within each primary artery, to provide an estimate of the severity of disease. In the case of the Qanadli index, a score <20 indicates a low-risk clot burden, whereas a score ⩾20 indicates a high-risk clot burden, for which a patient may be referred for more aggressive management, including catheter-based therapy or surgical thrombectomy. The pulmonary arterial supply to the lungs can be quantified using dual-energy CT, whereby CT data are acquired using two different X-ray tubes at varying peak kilovoltages. Iodine has a different CT attenuation at varying kilovoltages, and so it is possible to selectively quantify the amount of iodine within the lungs after contrast injection. This technique can augment pulmonary embolism detection by 1% [18]. While this seems a small percentage, the technique has additional advantages: it is also a useful tool in assessing change every time in the case of high-risk pulmonary embolism, and has been

shown to depict microvascular angiopathy in patients with coronavirus disease 2019 pneumonia [19]. A detailed description of the appearance of each pulmonary arterial pathology can be found in the recent review by Leitman and McDermott [20].

In summary, the field of cardiovascular CT has undergone substantial advancements, ranging from improvements in image quality to radiation dose reduction. These developments collectively contribute to more accurate and personalised diagnoses of cardiovascular disease, and an extension of the indications for its use.

Thoracic ultrasound

Thoracic ultrasound (TUS) is a noninvasive imaging method of increasing significance in visualisation of pleural and subpleural pulmonary diseases, as dynamic imaging is also possible. Point-of-care ultrasound is commonly used in the emergency room, in the intensive care unit and in general wards. This modality has many advantages: it is widely available, easily repeatable, cheap, portable, has no ionising radiation and provides rapid answers to clinical questions at the patient's bedside. Furthermore, TUS shows a steep learning curve [21] and in some cases (trauma, lying patients) provides higher sensitivity than CXR and even CT scans [22–24]. TUS allows quick differentiation of respiratory symptoms, diagnosis of lung and pleural diseases, monitoring of treatment, prognosis of the disease outcome and guidance for some interventional procedures. Furthermore, TUS is used by doctors of various specialties (respiratory, critical care and emergency medicine), not being any longer restricted to the domain of radiologists.

Despite many advantages, this imaging modality also has limitations; for example, only abnormalities that attach visceral pleura can be visualised (even a small rim of normal lung or air in the pleural cavity reflects ultrasound waves and enables visualisation). Furthermore, in sitting patients, only about 70% of the lung surface can be examined, and mediastinal and diaphragmatic pleura are in the majority of cases beyond access by TUS. Additional limitations include obesity, emphysema and bad patient condition, such as lying patients and those with dressings, when the visibility might be decreased.

TUS is usually performed with a low-frequency curved-array abdominal transducer (convex probe, 2–5 MHz), a high-frequency linear-array transducer (6–15 MHz) or a phased-array cardiac transducer (1–5 MHz) in supine and sitting (from back) positions. Convex probes provide a larger view and good penetration. High-frequency linear probes ensure good resolution for pleural surface and abnormalities in chest wall. The ultrasound transducer is first positioned on the chest wall perpendicular to two adjacent ribs and also in the intercostal space. While examining patients, all the available lung areas should be scanned and the findings described using one of the lung ultrasound protocols available (assessment of 6–18 or even 72 lung zones) [25, 26]. In dyspnoeic patients, the BLUE (bedside lung ultrasound in emergency) protocol is commonly used. The patient is examined in supine position and each lung is scanned in three areas: the upper anterior, the lower anterior, and the PLAPS (posterolateral alveolar and/or pleural syndrome) points [27].

TUS relies on the direct visualisation of structures and interpretation of artefacts; therefore, for better visualisation of the artefacts it is recommended to switch off some filters in the ultrasound machine, *e.g.* tissue harmonic imaging and compound imaging [28, 29]. Most frequently, B-mode is used (creating a two-dimensional (2D) image); however, M-mode (motion mode, giving a 1D view of all structures along one ultrasound line) may provide significant information for assessment of lungs, diaphragm and big vessels.

Due to the physics of TUS, most (99%) of the waves are reflected back on striking the soft tissue and air interface; moreover, the ribs cause acoustic shadows, known as the "bat sign", as the ribs resemble the wings of the bat and the pleural line mimics the body of the bat (figure 5a) [30]. Therefore, the pleura can be visualised within the intercostal spaces only, where the pleural line is a hyperechoic line representing the interface of the parietal and visceral pleura. In B-mode, normal lung pattern involves lung sliding, which shows the movement between the two pleural layers (visceral pleura against parietal pleura on the inner chest wall) [26]. In M-mode, normal lung creates the "seashore sign", in which the pleura and the overlying structures appear as horizontal echogenic lines, while the underlying lung gives a sandy appearance (figure 5b) [31].

The signs that are most frequently observed in TUS include vertical pleura artefacts (mainly B-lines), consolidation and pleural effusion (figure 5d–f). These findings are associated with increasing amounts of fluid in the lungs, increased lung density and decreased lung aeration. B-lines (often called "comet-tail sign") are vertical hyperechoic lines extending down from the pleural line to the edge of the screen without fading, in synchrony with lung sliding, obscuring the horizontal A-lines (figure 5d). B-lines are present in

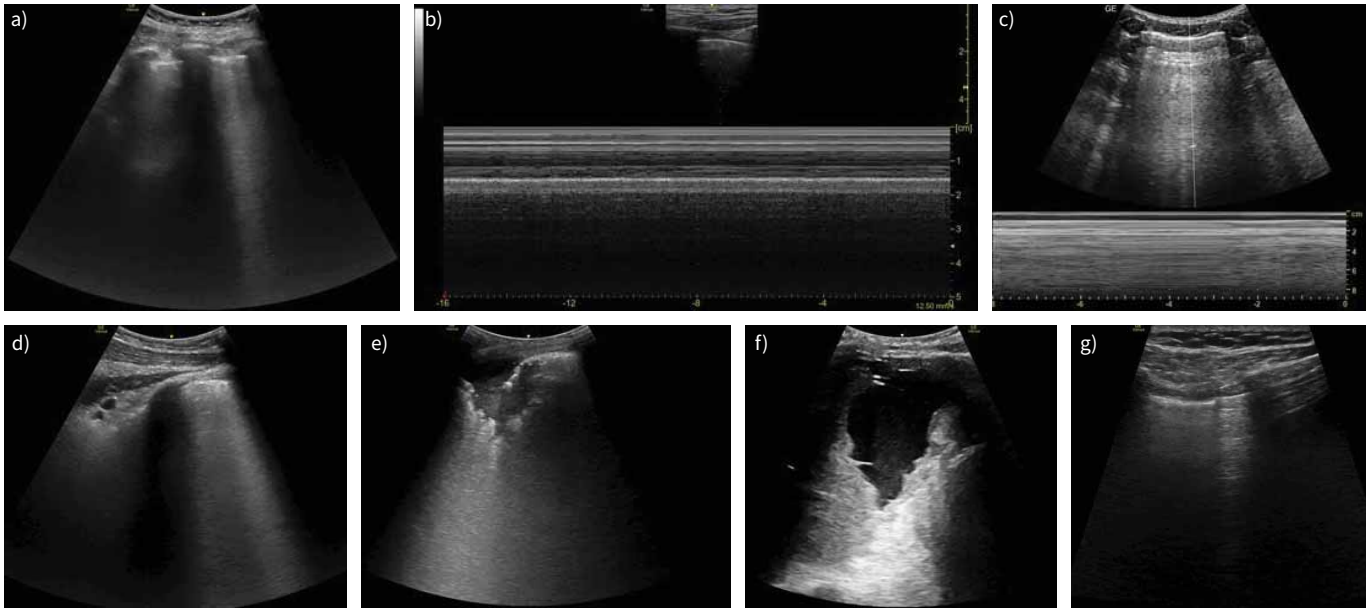

FIGURE 5 Typical signs on lung ultrasound. a) Bat sign. b) Seashore sign. c) Barcode/stratosphere sign. d) B-line. e) Consolidation. f) Pleural effusion. g) Lung point in pneumothorax.

heart failure, cardiogenic and noncardiogenic pulmonary oedema, ARDS, interstitial lung diseases and pneumonia; in healthy people at the lung bases, they exclude pneumothorax [31, 32]. Lung consolidation is defined as a subpleural echo-poor region or region with tissue-like echotexture (resembling liver parenchyma), which can be observed in pneumonia, malignancy, pulmonary embolism, atelectasis and lung contusion (figure 5e) [32]. The signs that allow differentiation of underlying pathology are described elsewhere [25]. TUS is an excellent imaging method to identify even small amounts of pleural effusion, allowing classification, volume quantification and estimation of aetiology and outcome [33]. It is highly recommended to perform all pleural procedures for fluid under ultrasound guidance, as it reduces the risk and cost of iatrogenic complications.

Lung ultrasound is an appropriate, effective and safe technique by which an experienced radiologist/pulmonologist can perform ultrasound-guided percutaneous biopsy of peripheral subpleural lesions, even small ($\leqslant$2 cm) lesions [34]. In addition, some studies have shown that contrast-enhanced ultrasound of peripheral nonsmall cell lung cancer (NSCLC), especially in squamous cell carcinoma, can demonstrate microvessel density within the tumour, which can be used as a quantitative parameter for treatment surveillance and may differentiate between benign and malignant peripheral pulmonary lesions [35, 36].

Both in the normal lung and in pneumothorax, A-lines may appear: horizontal echogenic lines parallel to the pleura at equal intervals, due to repetition artefacts of the parietal pleura. A-lines are better appreciated with a linear transducer.

Chest ultrasound is frequently performed to detect pneumothorax, especially in trauma and critical care patients but also after interventional procedures such as lung biopsy. Specific features described in pneumothorax are a lack of lung sliding, the absence of B-lines and identification of a lung point (figure 5g), and in the M-mode, the “barcode” or “stratosphere” sign (figure 5c). Lung sliding is also absent in pleural effusion, pleurodesis, severe acute lung injury, prior thoracic surgery, atelectasis, lobar consolidation, and with large parenchymal tumours [37].

There is also increasing evidence that ultrasound supports the assessment of diaphragm function (assessment of mobility and thickness), chest wall abnormalities (malignant infiltration or rib fractures), fluid overload and heart dysfunction. Detailed description is beyond the scope of this review. Although there is not sufficient scientific evidence to translate ultrasound findings to clinically meaningful outcomes in many of these situations, keeping in mind the significance of the data that TUS may provide, this imaging modality should be a must-have tool for lung imaging in daily practice.

Among the new achievements in TUS, we should list contrast-enhanced ultrasound and elastography. Contrast-enhanced ultrasound is a real-time dynamic imaging technique that assesses contrast enhancement patterns in lungs, is safe in renal failure, and helps in detection of neoplastic lesions (enhancement in arterial phase) and identification of necrotic areas, which is beneficial in TUS-guided procedures [38]. Ultrasound elastography quantitatively assesses tissue stiffness by measuring the degree of distortion by application of an external force (shear waves). It might be helpful in the detection of malignant disease [39].

Thoracic MRI

MRI is not just a picture-producing method giving information about morphology, we can also gain a lot of tissue-characterising, functional and metabolic data [40]. The atom used is hydrogen (containing just one proton), which occurs in an abundant quantity in the tissues of living beings (fluids, fat, muscles and viscera), but not in the air, with fewer and more oriented hydrogen protons in bones (MRI does not work with ionising radiation as an exciting energy of those). In a constant magnetic field (0.5–3.0 Tesla (T)), a radio wave impulse is given, exciting hydrogen atoms. When they relax again, they radiate back the energy, which can be detected by antennas (coils) point by point, exactly showing their 3D positions. Thereafter, a powerful computer works up this data, creating pictures. However, MRI is not that useful for imaging lung tissue itself, because alveolar walls are too tiny to be delineated.

Hazards

Naturally, all known everyday precautions should be performed around/in the big magnet! Additionally, thoracic investigations are often required in patients with pacemakers. The investigators should be aware of the type of pacemaker (whether it is compatible with MRI or not) and/or presence of a cardiologist can be compulsory (inspecting while switching off and on the pacemaker).

Movement, due to breathing and pulsing heart and blood vessels, can be another problem. There are respiration and pulse controlling sequences to be performed: cardiac and respiratory gated MRI studies. These types of imaging need a longer scanning time.

Anatomy

The anatomy of the thorax is suitable for MRI in conventional frontal, sagittal and even axial planes (resembling CT slices, multiplanar and 3D). MRI can visualise the thoracic wall, the diaphragm and the mediastinal space. Within the thoracic wall, we can see the skin, muscles, ribs and vertebra, and frontally the sternum. The diaphragm, covered with pleura, separates the thoracic cavity from the abdominal one. Mediastinal space is found between the lungs, containing the oesophagus, trachea, heart, large vessels, lymph nodes and thymus. Between these organs, the "filling material" is fatty tissue and/or loose connective tissue. There are several anatomical classifications for the subdivisions of mediastinum. The most used are "superior", "anterior", "middle" and "posterior".

Indications

CT has better spatial resolution but MRI resolution in terms of tissue differentiation is better. This increases diagnostic certainty and helps in surgical planning of interventional procedures (figure 6a).

Many problems can be better resolved with MRI compared with other types of investigating methods. For example, MRI can be used for distinction of abscesses (intra- or extrapulmonary) by diffusion-weighted imaging (DWI) sequences. In cases of chylothorax, MRI can show the location of its origin, *i.e*. leakage of the thoracic duct.

MRI is a useful tool for investigating most common masses in the mediastinum. In the anterior and superior mediastinum, masses may be of thyroid, thymus, lymphoma, germ cell, vascular or lymphatic (cystic) origin; in the middle part of the mediastinum, there may be cysts or lymphomas; and in the posterior, masses are mostly of neurogenic origin.

With respect to specific masses, the role of MRI is important for hilar/mediastinal lymph node masses (metastases, Hodgkin and non-Hodgkin lymphomas, tuberculosis or sarcoid masses). In cases of extreme enlargement of the thyroid gland and spreading towards the mediastinum (retrosternal goitre, even intrathoracic, which is not connected), MRI helps in the planning of surgical removal. MRI helps in decisions regarding enlargements/tumours of the thymus (myasthenia gravis). For the parathyroid, in cases of tumours or overproduction, nuclear medicine affords the correct diagnosis, but before an operation, the more precise (3D) localisation possible by MRI can help. Germ cell tumours can occur in the anterior mediastinum, and can form teratomas (benign and malignant), germinomas, embryonal choriocarcinomas, *etc*. Again, MRI can be an important diagnostic aid. Masses of neural origin can be benign (*e.g.*

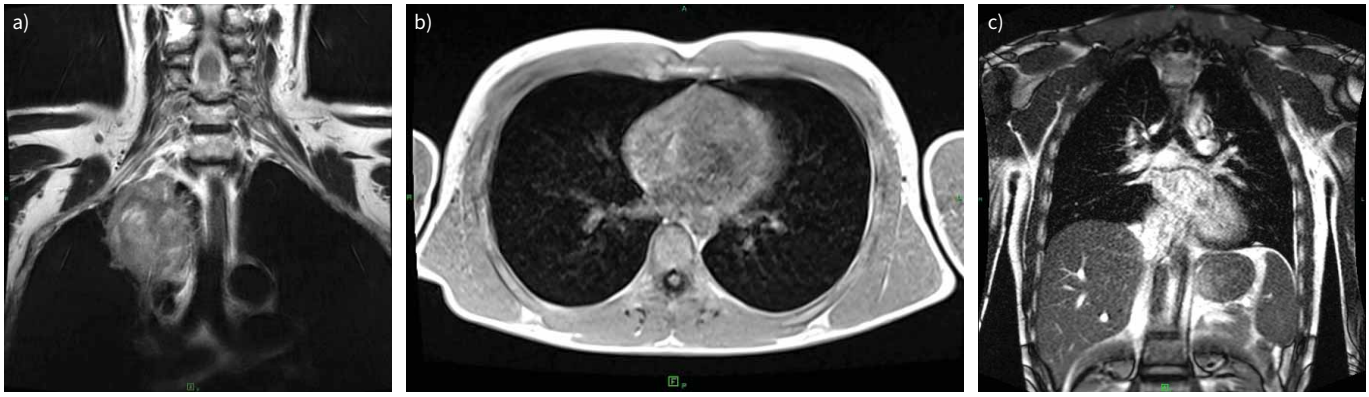

FIGURE 6 Magnetic resonance imaging (MRI). a) Axi T2 PROPELLER MRI scan of a 68-year-old patient demonstrated right upper lobe Pancoast tumour, with infiltration of the adjacent soft tissues. The tumour appears to be separated from the superior vena cava and the right brachiocephalic vein, as well as from the brachial plexus, by a narrow band of fat, while infiltration of the right subclavian artery has arisen. b and c) Low-field (0.55 T) MRI study of the lung with b) axial T1 VIBE TRA and c) coronal T2 TRUFI P2 FS sequence for the study of diaphragmatic motion during free breathing.

neurofibromas or ganglioneuromas) or malignant (*e.g.* neurofibrosarcomas or ganglio/neuroblastomas) and occur mostly in the posterior mediastinum (some are paravertebral). MRI has an important role in pointing out spreading and/or interconnection with intraspinal spaces.

Diaphragm hernias are mostly studied with traditional imaging methods, but in babies (Bochdalek hernias) they may be an indication for MRI. Nowadays, low-field (0.55 T) MRI for the study of lung and diaphragmatic motion is under investigation (figure 6b and c).

In this list of MRI indications, we also must not omit the role of MRI in searching for bone metastases, invasions and bone marrow anomalies, where MRI is very strong and reliable, not only for local invasions but also for general metastatic processes (in the ribs, sternum and vertebra). If there is suspicion of a generalised myeloma, multiplex MRI has an exclusive role.

Acute mediastinitis is a serious state with a high death rate if correct diagnosis is delayed. The most alarming is when it occurs after forced vomiting (Boerhaave syndrome) or after endoscopic manipulation/oesophagus operation. But if it spreads in a larval way (descending necrotising mediastinitis, odontogenic or oropharyngeal) or comes from a sternal osteomyelitis, MRI helps in stating the correct diagnosis. Chronic fibrosing mediastinitis can occur with autoimmune diseases, *Histoplasma* or tuberculosis infections, sarcoidosis, or after irradiation and some medications [41].

Strengths

MRI is a preferable investigation method to CT because it does not use ionising X-rays for producing pictures and has a superior role in diagnosing thoracic problems. MRI is a multiparametric investigation method, providing more detailed, multiple, multivarious data about soft tissues. These can all result in a more complex interpretation while establishing a more correct diagnosis.

Limitations

MRI investigations have a general limit as mentioned in the earlier “Hazards” section. The main problem can be a non-cooperative patient, *i.e.* they may be claustrophobic, agitated or tremorous. These are more impedimental factors than for CT investigations, but they can be overcome. Inbuilt metallic articles, if magnetisable, can forbid MRI investigation, or the artefacts caused may make the collected data uninterpretable or false. Be aware that tattoos can have ferrous or other magnetisable metals that can cause severe burnings in the skin.

Thoracic intervention

Percutaneous image-guided lung intervention includes transthoracic needle biopsy, thermal ablation, fiducial placement, tunnelled pleural catheter placement, bronchial artery embolisation and catheter-directed therapy for pulmonary embolism and is made possible by advances in CT, fluoroscopy

and ultrasound technology, as well as the proliferation of new devices in the field. Interventional radiology has many options to offer patients with lung cancer, haemoptysis and pulmonary embolism. The indications, strengths and limitations of the related diagnostic and therapeutic procedures will be described in this section.

CT-guided lung biopsy

Tissue sampling of pulmonary lesions is crucial to the assessment of patients with a suspected lung malignancy and allows for diagnostic confirmation of a lung cancer or metastasis, and for molecular subtyping [42, 43]. CT-guided biopsy of solitary pulmonary nodules has a reported diagnostic accuracy of 92.9%, with a sensitivity and specificity of 95.3% and 95.7%, respectively. CT-guided lung biopsy is contraindicated in the setting of an irreversible bleeding diathesis. The most common complication is pneumothorax requiring chest drain insertion, which occurs in 13.1–16.7% of patients [44].

Biopsy provides a means not only to obtain a diagnosis but also to pursue molecular testing to provide treatment specific to the tumour subtype. Lung biopsy now has renewed importance in the characterisation of lung cancers that are potentially suitable for immunotherapy [45].

Thermal ablation

The standard of treatment for early-stage NSCLC is surgical resection [46]. However, significant medical comorbidities and poor cardiopulmonary reserve often preclude surgical intervention. Percutaneous ablative therapies also offer a treatment option for patients with oligometastatic pulmonary disease [47].

Thoracic ablative techniques use CT guidance to percutaneously direct an ablation probe within, or close to, the lesion so that thermal energy may be administered to the tumour, aiming for a 1-cm zone of surrounding normal tissue to achieve a clear margin [48]. Modalities currently in use include radiofrequency ablation (RFA), microwave ablation (MWA) and cryotherapy.

Indications

Patient selection for lung tumour ablation requires the input of a multidisciplinary team [49]. Given the epidemiological profile of lung cancer and its associated risk factors, in particular smoking [50], patients may present with comorbidities that prohibit surgical intervention and therefore alternative localised therapies may be considered [51]. Percutaneous thermal ablation is a useful salvage tool in the context of primary lung carcinoma recurrence following surgery, chemotherapy or radiotherapy [52, 53]. Thermal ablation provides an alternative to surgery for medically comorbid patients with oligometastatic extrathoracic cancer [54]. There is no specifically defined number of lesions which may be ablated; however, most centres treat patients with five or fewer metastases.

Outcomes

Primary lung carcinoma

Analysis of outcomes for ablation as a treatment for stage I NSCLC to date is limited by size, concomitant treatment and population heterogeneity [54]. Recurrence rates after RFA of stage I NSCLC are reported in 12 retrospective studies; the aggregate rate of local progression is 24% (95 out of 403 patients) [55–64]. Reported 3- and 5-year survival rates range from 36% to 88% [57, 59, 61, 64] and from 19% to 27%, respectively [57, 64].

Data on long-term survival for stage I NSCLC treated with MWA include 10 retrospective studies that report an aggregate local recurrence rate of 24% for lesions with an average size of 2.3 cm. Reported 2- and 5-year survival rates are 62–94.1% and 16–58.1%, respectively [65–70]. Data regarding cryoablation in lung carcinoma are currently limited.

One of the frequently reported benefits of thermal ablation in the lung is the ability to preserve lung function [71]. Ambrogi *et al*. [55] demonstrated no significant worsening in results from pulmonary function tests carried out 6 months after lung tumour ablation when compared with baseline pulmonary function tests carried out prior to the procedure.

Oligometastases

Outcome analysis in the setting of oligometastatic disease is subject to similar limitations to that of early-stage NSCLC. However, thermal ablation can achieve good control of tumour progression while avoiding the morbidity associated with thoracotomy [72]. Local tumour control is reported to have been achieved in the majority of patients treated with MWA of colorectal metastasis, with an aggregate local

recurrence rate of 9.8% [73–79]. Only one study has reported long-term survival: in a group of 50 patients with 90 lesions, 2- and 5-year survival was reported to be 98% and 90%, respectively [77].

Complications

The reported rate of major complications for thermal ablation is 9.8% and includes pleuritis, pneumonia, lung abscess, haemorrhage, and pneumothorax requiring pleurodesis. Rarer major complications include bronchopleural fistula, tumour seeding, and nerve or diaphragmatic injury (<0.5% incidence). Pneumothorax requiring thoracostomy after RFA had an incidence of 22.1% in a retrospective study of 1000 patients [80]. The reported mortality rate after RFA for lung tumours is 0.4%. Nerve injury is rare and can affect the phrenic, brachial, left recurrent laryngeal, and intercostal nerves, as well as the stellate ganglion [81].

Fiducial placement

Fiducials are radiopaque markers inserted under image guidance into the vicinity of a tumour to aid its localisation. The applications in lung cancer treatment include image-guided radiation therapy and minimally invasive thoracic surgery.

Stereotactic body radiotherapy has emerged as a therapeutic option for NSCLC [82]. Lung tumours are prone to motion artefact. Fiducial markers provide a method of increasing dosing accuracy. This allows the stereotactic body radiotherapy system to track tumour position throughout respiration, ensuring focused radiation dose delivery to the tumour [83].

Surgical localisation for non-palpable lesions

Radiologically placed markers may also be used to aid localisation of small pulmonary lesions during minimally invasive thoracic surgery in order to increase the chance of complete resection and avoid conversion to thoracotomy. The markers are placed preoperatively under CT guidance adjacent to the target lesion, facilitating intraoperative identification of the area to be resected [84–86]. There have been several reported techniques for marking non-palpable lesions, including hook wires, vascular coils and injected technetium. Complications associated with fiducial placement include pneumothorax, and very rarely fiducial embolisation, migration and parenchymal haematoma. Migration of markers has been reported in 1.7–25% of patients [87].

Bronchial artery embolisation

Bronchial artery embolisation is a minimally invasive technique used in the management of moderate recurrent or massive haemoptysis. The treatment can be used to occlude or cause stasis in hypertrophied bronchial arteries resulting from chronic lung disease, tumour-related hypervascularity, aneurysm formation or arteriovenous malformations [88–90]. Embolotherapy of the hypertrophied bronchial artery is performed using either gelatin sponge, polyvinyl alcohol particles, microspheres, liquid embolic agents such as *N*-butyl-2-cyanoacrylate, and microcoils. The success rate of bronchial artery embolisation ranges from 60% to 90% [91, 92]. Recurrence is particularly noted in diseases such as tuberculosis, bronchiectasis, aspergilloma and bronchogenic carcinoma. Complications include non-target embolisation to the oesophagus or the spinal artery [93].

Catheter-directed therapy for pulmonary embolism

Catheter-directed thrombolysis

Catheter-directed thrombolysis (CDT) involves the placement of catheters directly into a clot in one or both pulmonary arteries and infusing low doses of thrombolytic drug. CDT may be performed using a simple infusion catheter or an ultrasound-assisted endovascular system infusion catheter. The advantage of CDT is the use of thrombolytic agents (*e.g.* alteplase) in relatively low doses, typically ranging 4–12 mg per lung, with infusion durations of 4–24 h. This may translate into a lower risk of major bleeding even in those considered high risk. Given the usual infusion duration of several hours, patients needing immediate restoration of haemodynamics may not be ideal candidates for CDT.

In a prospective, randomised controlled trial (ULTIMA), 59 patients were randomised to either unfractionated heparin alone or ultrasound-assisted CDT plus unfractionated heparin, and the latter group demonstrated improved right ventricle (RV) to left ventricle (LV) diameter ratio in the first 24 h, with a very low risk of bleeding [94]. A single-arm, prospective trial of ultrasound-assisted CDT additionally showed early reduction in pulmonary pressures and obstruction index, with a 10% moderate bleeding rate but no intracranial haemorrhage [95].

Mechanical thromboaspiration

The technique of mechanical thromboaspiration involves placing an 8–24-Fr catheter selectively into one or both pulmonary arteries and directly aspirating a thrombus, allowing immediate restoration of flow. This can be used in combination with CDT. The advantage of mechanical thromboaspiration is that it may be used in patients with high bleeding risk or in those with contraindications to systemic anticoagulation. In the setting of high-risk pulmonary embolism, where rapid restoration of perfusion is preferred to reduce RV end-diastolic pressure and offload the RV, mechanical thromboaspiration is considered when the patient has a relative or absolute contraindication to systemic thrombolysis. CDT is used as an adjunct in this situation. Additionally, mechanical thromboaspiration is also considered an alternative for surgical embolectomy when the patient has multiple comorbidities.

EXTRACT-PE was a prospective multicentre single-arm study of 8-Fr catheter-directed thromboaspiration [96]. The treatment achieved a significant reduction in RV/LV ratio at 48 h ($p<0.0001$) and, in 98.3% of cases, this was achieved with no intraprocedural thrombolytic use and very low device-related complications (1.7%).

Larger-bore devices have been developed that aim to aspirate embolic material with manual suction applied with use of an aspiration syringe. A prospective multicentre single-arm study (FLARE) demonstrated that a significant RV/LV ratio reduction at 48 h was achieved. Additionally, 98% patients received no thrombolytic drugs, there was 0% device-related complications, and 41.3% patients required no intensive care unit stay [97]. The same device was compared to other therapeutic options such as thrombolysis or anticoagulation alone in an observational study. This confirmed a lower complication rate in the thromboaspiration group, whereby in-hospital mortality occurred in 1.9% of patients treated with catheter thromboaspiration compared to 29.5% of patients treated with systemic thrombolysis or anticoagulation [98].

A large international registry has also reported the outcomes of 800 patients: the FLASH registry data describe a low 30-day mortality of 0.8%, and reduction of the RV/LV ratio from 1.2 to 0.98 at 48 h with a 1.8% incidence of major adverse events, *e.g.* access-related haematoma and acute anaemia [99]. What remains to be seen is the comparative value of catheter-directed thromboaspiration to surgical embolectomy, and the best time-point at which to intervene with CDT, to maximise good patient outcomes.

Summary of interventions

In summary, image-guided thoracic intervention has vastly improved the minimally invasive management of patients with thoracic malignancy, thoracic vascular haemorrhage or thromboembolism. The advantages of image-guided thoracic intervention include safe and accurate diagnosis in the case of biopsy of palliative pleural drainage, effective guidance of thermal ablation, avoidance of surgical intervention in the case of patients with multiple comorbidities and pulmonary haemorrhage or thromboembolism, and successful localisation of lung tumours prior to irradiation or surgery.

Nuclear medicine imaging in pulmonary diseases

This section briefly summarises the role of traditional nuclear medicine and PET imaging in the diagnosis (and therapy) of pulmonary diseases.

Traditional nuclear medicine

Ventilation/perfusion (V'/Q') scanning is the most frequently performed test in traditional nuclear medicine. The ventilation phase visualises the airflow distribution, and the perfusion phase shows the blood flow distribution in the lungs. The main purpose of a V'/Q' scan is to evaluate suspected acute or chronic pulmonary embolism, particularly in patients for whom CT angiography is inconclusive or contraindicated, such as pregnant women or patients with renal insufficiency or severe contrast allergy. Furthermore, perfusion imaging also allows calculation of relative lung perfusion before lung volume reduction surgery and lung transplantation.

Imaging starts with the ventilation scan, during which technetium-99m (^{99m}Tc)-labelled radiopharmaceuticals (radioactive xenon or krypton can also be used) are inhaled through a nebuliser *via* a mouthpiece for a few minutes. The perfusion phase of the scan starts with the intravenous injection of ^{99m}Tc-labelled macroaggregated albumin. The administration of the radiopharmaceuticals is immediately followed by planar imaging of the lung with four to eight views and single-photon emission computed tomography (SPECT), most often performed together with CT.

Thrombi typically block pulmonary arteries, causing characteristic peripheral wedge-shaped lobar, segmental or subsegmental perfusion defects with normal ventilation (V'/Q' mismatch). Pulmonary

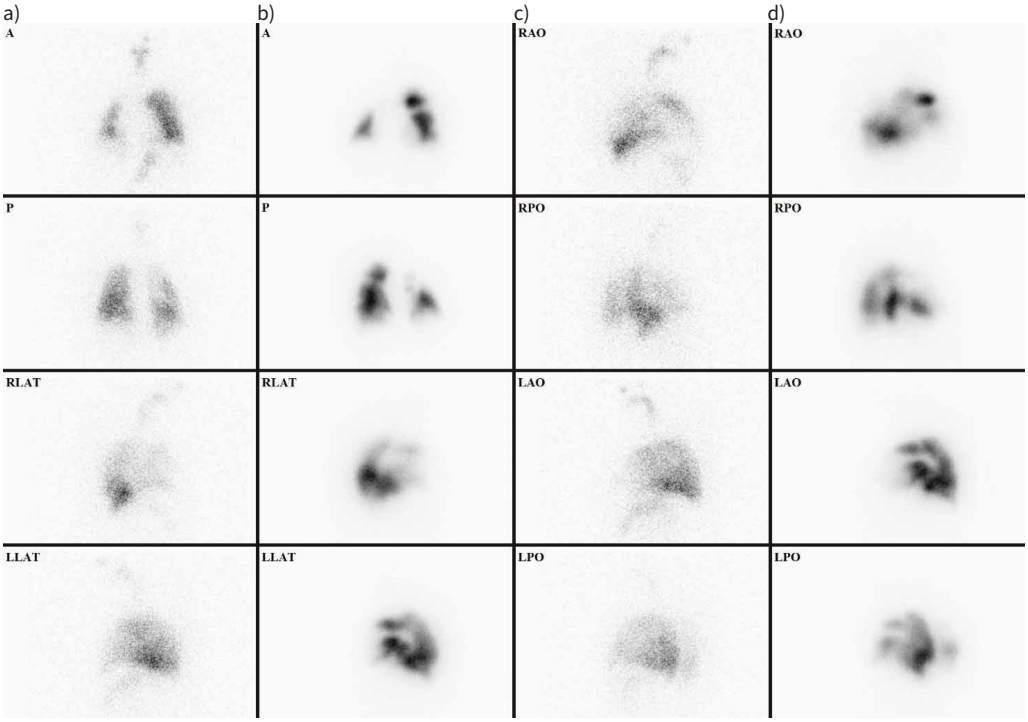

FIGURE 7 Ventilation/perfusion (*V'*/*Q'*) scan of a 56-year-old female patient with progressively worsening dyspnoea. a and c) ventilation images; b and d) perfusion images. There are multiple characteristic peripheral, wedge-shaped segmental-subsegmental perfusion defects with normal ventilation pattern suggesting *V'*/*Q'* mismatch, which confirms the diagnosis of pulmonary embolism. A: anterior; P: posterior; RLAT: right lateral; LLAT: left lateral; RAO: right anterior oblique; RPO: right posterior oblique; LAO: left anterior oblique; LPO: left posterior oblique.

embolism can be considered less likely if the form of the defect does not follow the pulmonary vascular anatomy. The diagnosis of pulmonary embolism cannot be confirmed if the distribution of the radiopharmaceuticals in the lungs is homogeneous, the perfusion exceeds ventilation (*V′*/*Q′* match or reverse mismatch, *i.e.* primary ventilation abnormalities, sometimes with hypoxic vasoconstriction, *e.g.* COPD or asthma), or a *V′*/*Q′* defect with radiographic features is found (triple match, *e.g.* pneumonia, tumour or atelectasis) (figure 7) [100–102].

Traditional nuclear medicine imaging also provides the possibility of determining whether there is reflux into the respiratory tract. To achieve this, patients are required to consume a liquid meal that is mixed with radiopharmaceuticals, which are not absorbed by the gastrointestinal or pulmonary mucosa. In case of aspiration, the appearance of the radiopharmaceutical in the lungs can be depicted [102, 103].

PET/CT imaging in NSCLC

PET/CT imaging plays an essential role in the management of NSCLC. Fluorine-18 (^{18}F)-labelled 2-fluoro-2-deoxy-D-glucose (FDG) is the most commonly used PET tracer in oncology. FDG is a glucose analogue that accumulates in tumour cells *via* membrane glucose transporters (mainly GLUT-1 and GLUT-3) due to abnormally increased metabolism. However, this phenomenon is not specific to malignancies, so other conditions, such as inflammatory or infective processes (*e.g.* granulomatous diseases such as sarcoidosis and tuberculosis, or aspergillosis, abscesses or interstitial lung diseases), can also show increased FDG accumulation, leading to false-positive results. In addition, FDG uptake is variable in different lung histological subtypes: squamous cell carcinoma usually has higher FDG avidity than adenocarcinoma, while pulmonary neuroendocrine tumours (NETs) and mucinous neoplasms most often show low FDG accumulation [104].

PET/CT has an established role in characterising solitary pulmonary nodules, staging, identifying a target for biopsy, therapy planning, treatment monitoring, prognostication, and detecting residual tumours or tumour recurrence [102].

The characterisation of indeterminate solitary pulmonary nodules has become one of the main indications of FDG-PET/CT; it has much higher sensitivity and is preferable to CT. FDG-PET/CT can efficiently differentiate between benign and malignant lesions by showing whether the nodule is hypermetabolic. It is suggestive of malignancy if the standardised uptake value is >2.5. According to the American College of Chest Physicians (ACCP) guidelines, PET/CT is not indicated for solitary pulmonary nodules of <8 mm. This threshold was defined because the spatial resolution of PET limits the evaluation of smaller lesions. FDG-PET/CT should also be avoided in the characterisation of non-solid nodules to prevent false-negative results (*e.g.* due to atypical adenomatous hyperplasia, carcinoma *in situ* or minimally invasive carcinoma) and false-positive results (*e.g.* due to inflammation or infection) [102, 105]. Small solitary pulmonary nodules (<15 mm) located in the lower lobes can also be false negatives due to motion artefacts; in these cases, respiratory gating is highly recommended [106].

Another common indication for FDG-PET/CT is the staging of pulmonary malignancies. Based on numerous studies, FDG-PET/CT is considered the best imaging technique for T staging of NSCLC because it provides essential information on mediastinal and chest wall infiltration and differentiation between tumour and peritumoral atelectasis. Furthermore, it can accurately determine the exact location of the primary tumour. It has also been demonstrated that FDG-PET/CT is superior to contrast-enhanced CT in nodal staging. While lymph node size (short-axis diameter >10 mm) is the only criterion to determine metastatic disease on CT imaging, FDG-PET/CT provides additional metabolic information that can help identify smaller metastatic lymph nodes or enlarged, benign ones [107]. FDG-PET/CT has also been reported to be the best imaging technique for detecting distant metastases; they are often missed or equivocal on conventional imaging. Detecting brain metastases with PET/CT is often tricky because glucose is the primary substrate of brain metabolism, so brain activity is usually very high. That is why brain CT (or MRI) is always part of staging. The detection of adrenal metastases could also be challenging because they can be mistaken for adrenal adenomas. In addition, lungs are a common site for metastases, and it is sometimes difficult to distinguish them from primary tumours (figure 8) [102, 108].

Imaging in pulmonary NETs

Pulmonary NETs are a heterogeneous subgroup, including low-grade (carcinoid tumour), intermediate-grade and high-grade malignant tumours (including small cell lung cancer and large cell neuroendocrine carcinoma). They express varying amounts of somatostatin receptors (SSTRs). High-grade pulmonary NETs are poorly differentiated; they often show low SSTR levels and high FDG avidity. Carcinoid tumours are well differentiated; they are rich in SSTRs and show lower glucose metabolism [109]. They generally cannot be detected with FDG-PET/CT; SSTR scintigraphy with radiolabelled somatostatin analogues (indium-111 (^{111}In)-labelled pentetreotide or ^{99m}Tc-EDDA/HYNIC-TOC) or SSTR-based PET tracers (gallium-68 (^{68}Ga)-labelled tetraazacyclododecane tetraacetic acid (DOTA) peptides (DOTANOC, DOTATOC or DOTATATE)) are used instead. PET tracers have multiple advantages compared with SSTR

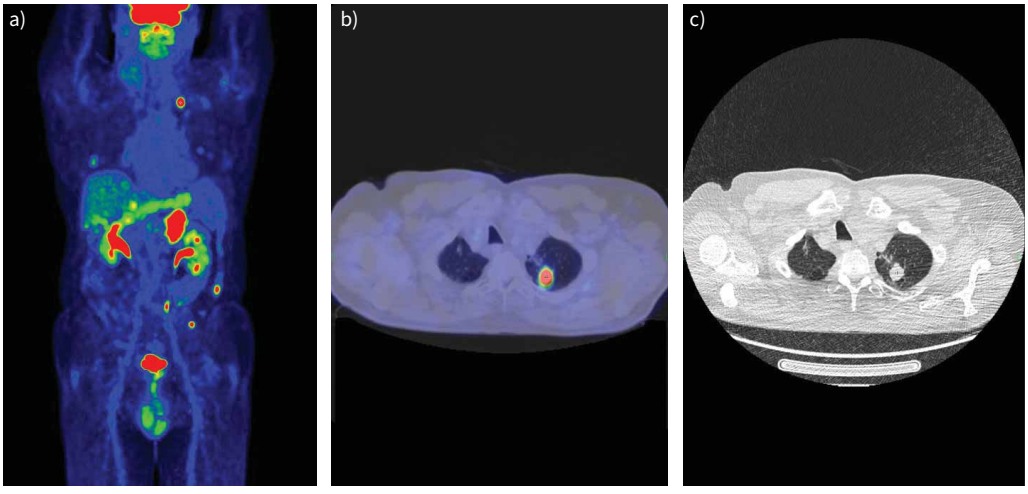

FIGURE 8 Staging of lung adenocarcinoma with 2-fluoro-2-deoxy-D-glucose positron emission tomography/computed tomography (FDG-PET/CT). a) PET image; b) fused image; c) chest CT. Images show the primary tumour in the left lung, multiple pulmonary inflammatory lesions and bilateral adrenal metastases.

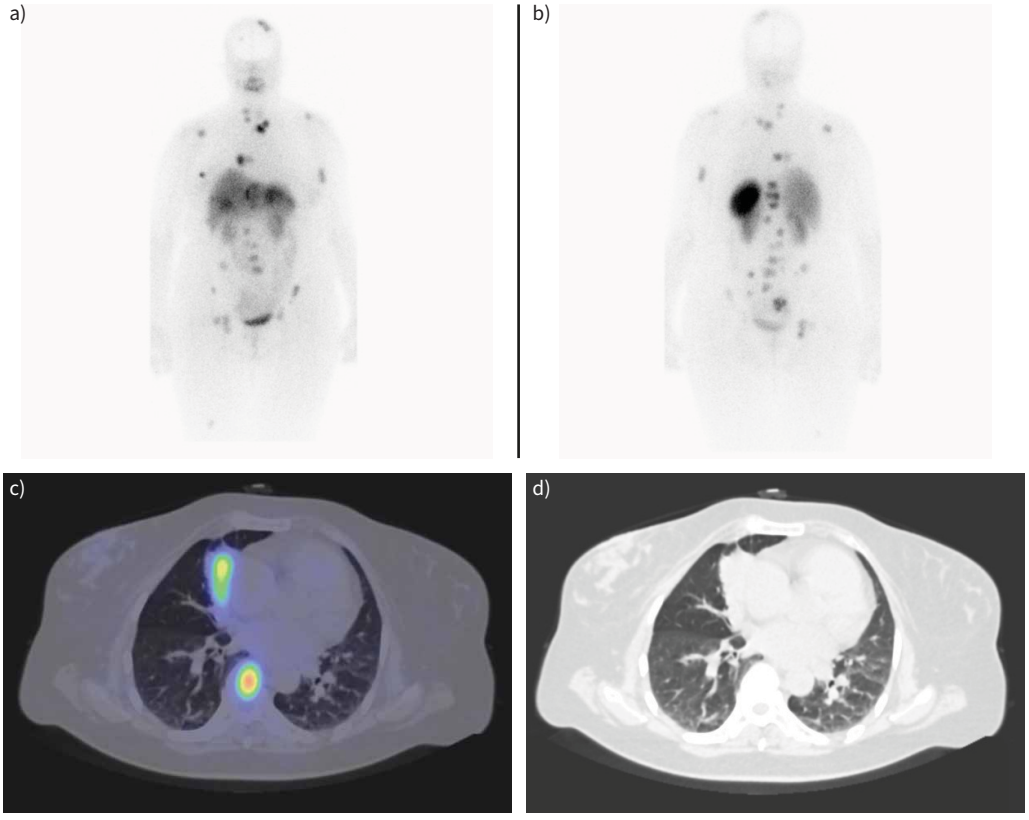

FIGURE 9 A 54-year-old female patient diagnosed with a lung carcinoid tumour underwent somatostatin receptor scintigraphy using a technetium-99m (^{99m}Tc)-labelled somatostatin analogue. a) Anterior and b) posterior whole body planar images display the primary tumour in the right lung, as well as solitary hepatic and breast metastasis and multiple bone metastases. c) Fused and d) computed tomography (CT) images from single-photon emission computed tomography (SPECT)/CT imaging of the patient depict the primary tumour in the middle lobe of the right lung and bone metastasis in the body of the seventh thoracic vertebra.

scintigraphy: they have a higher affinity for SSTRs, and PET has higher sensitivity and specificity than SPECT due to superior contrast and spatial resolution (figure 9) [102, 110].

Dihydroxyphenylalanine (DOPA) is an intermediate in catecholamine synthesis; labelled with ^{18}F (6-^{18}F-fluoro-L-dihydroxyphenylalanine), it is used in the evaluation of the dopaminergic nervous system and the detection of various malignancies, including well-differentiated NETs (*i.e.* also carcinoid tumours). NET cells show increased DOPA uptake because it is the substrate of the DOPA decarboxylase enzyme, which is overexpressed in NETs [102, 111].

The main indications of these PET tracers are the characterisation of pulmonary nodules with neuroendocrine activity, the staging of primary NETs, and the evaluation of therapy response. According to the European Society for Medical Oncology (ESMO), somatostatin analogues are preferred over DOPA for NET PET/CT imaging due to their superior properties [104].

Other PET tracers

In addition to the aforementioned tracers, numerous other radiopharmaceuticals are currently used in clinical practice or are the subject of intensive research (table 2). These radiopharmaceuticals can either be nonspecific, targeting intracellular processes such as proliferation, angiogenesis, hypoxia or apoptosis, or specific, showing affinity only to selected antigens.

PET/MRI imaging in pulmonary diseases

PET/MRI provides a comprehensive assessment of malignancies by merging functional and anatomical data while offering high-quality soft tissue contrast. However, many departments still have limited access to PET/MRI systems. Furthermore, pulmonary MRI can be challenging due to the low signal caused by

TABLE 2 Radiotracer types, with mechanisms and clinical applications

Radiotracer	Mechanism	Clinical application
^{18}F-FLT	Nucleoside analogue, incorporates into DNA, accumulation depends on the intensity of cell proliferation	Does not accumulate in inflammatory processes, differentiates inflammation (*e.g.* sarcoidosis or tuberculosis) from malignancy (possibly together with FDG) [102, 104]
^{11}C-MET	Amino acid analogue, accumulation depends on the degree of protein metabolism	Does not accumulate in inflammatory processes, differentiates inflammation (*e.g.* sarcoidosis or tuberculosis) from malignancy (possibly together with FDG) [102, 104]
Radiolabelled tumour angiogenesis and hypoxia markers	Can provide helpful information about the tumour vasculature, oxygen supply, and internal tumour microenvironment	Pre-monitoring the mentioned information could be helpful in determining the prognosis and in selecting appropriate and effective individualised therapy [102, 104, 112, 113]
FAPI	Targets FAP, which is a transmembrane glycoprotein overexpressed by activated fibroblasts in the tumour stroma	Diagnosing malignancies with strong desmoplastic reactions, such as lung cancer [104, 114]
Radiolabelled tyrosine kinase inhibitors (*e.g.* EGFR-targeting drugs) and PD-L1-targeted PET tracers		Pre-treatment imaging to predict response to therapy [102, 104]

^{18}F-FLT: 3′-deoxy-3′-^{18}F-fluorothymidine; ^{11}C-MET: L-methyl-^{11}C-methionine: FAPI: fibroblast activation protein inhibitor; FDG: 2-fluoro-2-deoxy-D-glucose; EGFR: epidermal growth factor receptor; PD-L1: programmed death-ligand 1; PET: positron emission tomography.

the low proton density of the lungs [101, 102, 115]. In addition, the attenuation correction is sometimes inaccurate. Moreover, the acquisition process is relatively slow, and motion artefacts are common (*e.g.* due to respiratory and cardiac motion) [101, 115].

The clinical applications of PET/MRI are yet to be fully established. Several studies have shown that FDG-PET/CT and FDG-PET/MRI have the same accuracy in assessing NSCLC staging, while PET/CT is better at detecting lung nodules (which can be missed in MRI due to motion artefacts) [102, 116–118]. MRI can provide additional information on the extent of primary tumour invasion (*e.g.* into pleura, chest wall and mediastinal structures), which can be crucial for determining resectability [119]. PET/MRI also allows for integrating brain MRI into the whole-body scan, thus improving the accurate detection of brain metastases [120]. PET/MRI and PET/CT with ^{68}Ga-labelled ligands have shown similar efficacy in detecting extrahepatic NETs, but further research is still needed [116, 118]. The role of PET/MRI in chronic inflammatory diseases (*e.g.* COPD, cystic fibrosis or interstitial lung diseases) is still being investigated [101].

Theranostics

When a different radionuclide is attached to the same carrier for imaging and therapy, it is called a theranostic. This approach enables targeted molecular therapy by utilising radionuclides with optimal decay characteristics. All the tissues in the radiation field are affected by external radiation therapy. However, the radiation source is internalised with a theranostic, which helps target specific malignant cells.

Certain theranostic radiopharmaceutical pairs have already been used in the therapy of pulmonary NETs, for example, ^{68}Ga-DOTATATE (already mentioned as a PET tracer) and lutetium-177/yttrium-90 (^{177}Lu-/^{90}Y)-labelled DOTATATE. ^{68}Ga-DOTATATE is used for the pre-treatment scan to confirm whether the tumours have targetable SSTRs. ^{177}Lu and ^{90}Y are beta-negative emitting isotopes; they enable targeted radionuclide therapy of NETs considered positive in the pre-treatment scan [102, 121, 122].

Nuclear medicine imaging in inflammatory lung diseases

Gallium-67 scintigraphy and imaging with radiolabelled and reinjected autologous leukocytes (known as white blood cell scintigraphy) used to be a significant tool for imaging of inflammatory and infectious lung diseases [102]. However, nowadays, they have been almost entirely replaced by FDG-PET/CT in clinical practice. Increased perfusion, capillary permeability and glucose uptake by activated immune cells lead to nonspecific FDG accumulation at the site of any inflammation or infection. Although the exact

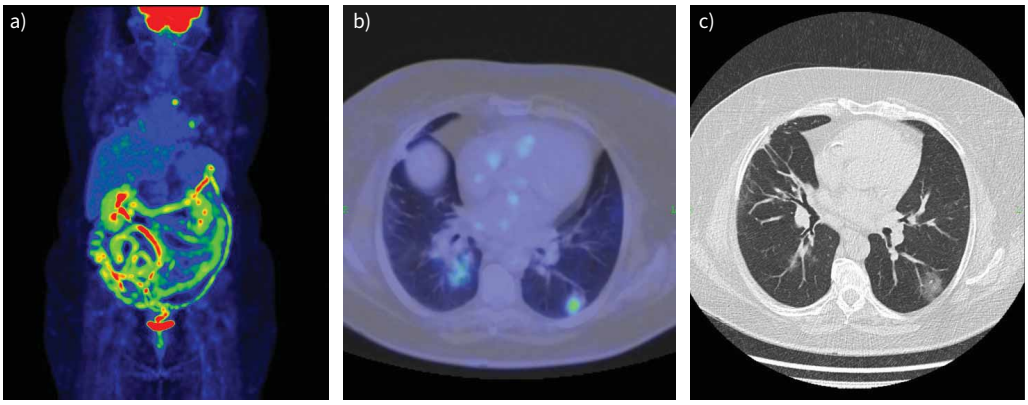

FIGURE 10 Coronavirus disease 2019 (COVID-19) pneumonia. 2-fluoro-2-deoxy-D-glucose positron emission tomography/computed tomography (FDG-PET/CT). a) PET image; b) fused image; c) chest CT. Images show bilateral, multiple, mainly peripheral, mildly/moderately active ground-glass opacities.

indications have yet to be officially defined, FDG-PET/CT is increasingly performed for detecting sarcoidosis and AIDS-associated opportunistic infections, as well as assessing metabolic activity in pulmonary fibrosis and tuberculotic lesions (figure 10) [102, 123–125].

There is intensive research into the characterisation of inflammatory diseases with new tracers. For example, radiolabelled antimicrobial and antifungal peptides [126], cytokines, antibiotics and antifungal drugs are under investigation. Viral infections could be detected by labelling viral particles or enzymes. Fibrosis could also be identified using radiolabelled fibroblast-targeting agents, for example in the early stages of interstitial lung diseases or radiation-induced lung fibrosis [102, 124, 125].

Conclusion

CXR is the basic imaging tool for the assessment of patients with respiratory symptoms and complaints, with a low radiation dose. In addition, digital chest tomosynthesis provides some of the tomographic benefits of CT but at lower cost and radiation dose than CT, improving the detection of subtle lung disease over conventional CXR. PCCT is a newly available imaging modality providing several advantages over conventional CT, such as lowered radiation dose and thinner slices of the lung (even 0.2 mm). TUS provides a supplementary imaging method for the assessment of pleural disease, certain peripheral lung disorders and diaphragmatic motion, among others. MRI also provides supplementary information on mediastinal diseases, and there is an emerging role of MRI in various lung diseases, such as nodule detection over a certain size, without radiation dose. In addition, the role of low-field (0.55 T) MRI studies in the chest is under investigation. Nuclear medicine imaging plays an essential role in the management of lung malignancies (and potentially of inflammatory or infectious lung diseases), and in the evaluation of pulmonary embolism. There are emerging studies in the field of radiomics and artificial intelligence, which is promising in providing a more accurate diagnosis and faster assessment in the future.

Key points

- Despite its limitations and the rapid development of various imaging methods/techniques, CXR remains the first, basic tool in the assessment of patients with respiratory symptoms and complaints.
- The role of TUS in lung imaging goes far beyond the assessment of pleural effusion and allows for rapid diagnosis of patients with respiratory symptoms such as dyspnoea.
- Progress in CT techniques such as PCCT has improved radiation dose efficiency, increased iodine signal, lowered doses of iodinated contrast material administration, and improved spatial resolution and spectral imaging, which are all beneficial in lung imaging.
- MRI is a valuable additional modality in certain clinical situations.
- Nuclear medicine imaging plays an essential role in the management of lung malignancies and infectious lung disease, and in the evaluation of pulmonary embolism.
- New techniques such as PCCT, radiomics and artificial intelligence can further help clarify the diagnosis and make a more accurate, faster assessment, and can be helpful tools for the radiologist and the clinician.

Self-evaluation questions

1. In which of the following contexts is CT-guided core biopsy contraindicated?
    a) Irreversible bleeding diathesis
    b) Primary lung carcinoma
    c) Metastastic disease
    d) When molecular tumour profiling is required
2. Which of the following can result from CT-guided lung ablation?
    a) Decline in lung function
    b) Pneumothorax in approximately 20% of patients
    c) Death in 10% of patients
    d) Local recurrence in 53% of patients
    e) Liver abscess
3. Which of the following treatments is best for symptomatic recurrent malignant pleural effusion?
    a) Talc pleurodesis
    b) Tunnelled pleural catheter placement
    c) Stereotactic body radiotherapy
    d) Repeated percutaneous pigtail catheter placement
4. Which of the following is often associated with catheter-directed therapy of pulmonary embolism?
    a) A decline in RV/LV ratio
    b) Death
    c) Pneumonia
    d) Access-related haematoma
5. What is the energy used for MRI investigation?
    a) Mechanical ultra waves
    b) Ionising electromagnetic waves
    c) Non-ionising radio waves
    d) X-ray waves
6. How can one overcome motion artefacts caused by breathing?
    a) During data collection, apply a breathing control system
    b) Bind the thorax tightly with a leather belt
    c) Narcosis is compulsory: the anaesthesiologist arrests the breathing
    d) Make more pictures in inspiration and then summarise those
7. What are the strengths of MRI during investigation of the thorax (mark all that apply)?
    a) During investigation, the lungs are shown perfectly
    b) MRI is a good method for soft tissue investigation
    c) MRI is the best investigating method for ventilation
    d) MRI can show bone metastases
8. What significant contribution of PCCT to coronary imaging is mentioned in this article?
    a) Increased radiation dose
    b) Decreased spatial resolution
    c) Higher motion artefact
    d) Minimising artefact due to calcified plaque
9. According to the NICE guidelines, when is CCTA recommended as a first-line investigation for patients with chest pain?
    a) High clinical likelihood of CAD
    b) New-onset stable chest pain
    c) Previous diagnosis of CAD
    d) Low likelihood of good image quality

Conflict of interest: E.M. Grabczak is a current member of the *Breathe* editorial board. C.A. Ridge discloses that Cobalt Charity has provided her institution with an education grant to fund a fellow, she is the RSNA Image Wisely co-chair, a ECR Thoracic educational committee member, a European Society of Thoracic Imaging educational committee member and *Lung Cancer Journal* radiology editor. She is the Director of AI Radiology limited (radiology reporting services). Á.D. Tárnoki is the current chair of the ERS Imaging group. The other authors declare that there is no conflict of interest.

Support statement: D.L. Tárnoki and Á.D. Tárnoki were funded by the Bólyai scholarship of the Hungarian Academy of Sciences; and ÚNKP-20-5 and ÚNKP-21-5 New National Excellence Program of the Ministry for Innovation and Technology from the source of the National Research, Development, and Innovation Fund. The project was implemented with support from the National Research, Development and Innovation Fund of the Ministry of Culture and Innovation under the National Laboratories Program (National Tumor Biology Laboratory (2022-2.1.1-NL-2022-00010)) Grant Agreement with the National Research, Development and Innovation Office.

References

1 Czibor S, Kiss FJ, Györke T. A fluorodezoxiglükóz pozitron-emissziós tomográfia/komputertomográfia szerepe a tüdőtumorok ellátásában [The role of fluorodeoxyglucose positron emission tomography/computed tomography in the treatment of lung tumours]. *Medicina Thoracalis* 2021; 74: 319–325.
2 Radiology Key. Imaging the chest: the chest radiograph. Date last updated: 4 July 2019. Date last accessed: 8 September 2023. https://radiologykey.com/imaging-the-chest-the-chest-radiograph/
3 Li Y, Jiang L, Wang H, *et al*. Effective radiation dose of ^{18}F-FDG PET/CT: how much does diagnostic CT contribute? *Radiat Prot Dosimetry* 2019; 187: 183–190.
4 Felson B. Fluoroscopy of the chest. *Dis Chest* 1955; 27: 322–329.
5 Kári B, Karlinger K, Légrády D, *et al.*, eds. Medical Imaging. Budapest, Semmelweis University and Budapest University of Technology and Economics, 2019. http://oftankonyv.reak.bme.hu/tiki-index.php?page=Orvosi_Posztgradu%C3%A1lis
6 Klein JS, Brant WE, Helms CA, *et al.* Brant and Helms' Fundamentals of Diagnostic Radiology. 5th Edn. Philadelphia, Wolters Kluwer, 2019.
7 Radiopaedia. Chest radiograph. Date last accessed: 8 September 2023. https://radiopaedia.org/articles/chest-radiograph
8 Nitrosi A, Borasi G, Nicoli F, *et al.* A filmless radiology department in a full digital regional hospital: quantitative evaluation of the increased quality and efficiency. *J Digit Imaging* 2007; 20: 140–148.
9 Leslie KO, Colby TV, Lynch DA. Anatomic distribution and histopathologic patterns of interstitial lung disease. *In:* Schwartz MI, King TE, eds. Interstitial Lung Disease. Shelton, People's Medical Publishing House, 2011; pp. 35–58.
10 Sathirareuangchai S, Yoshikawa A, Bychkov A. UIP/IPF. PathologyOutlines, 2023. www.pathologyoutlines.com/topic/lungnontumorUIP.html
11 Araki T, Nishino M, Zazueta OE, *et al.* Paraseptal emphysema: prevalence and distribution on CT and association with interstitial lung abnormalities. *Eur J Radiol* 2015; 84: 1413–1418.
12 Miller MM, Ridge CA, Litmanovich DE. Computed tomography angiographic assessment of acute chest pain. *J Thorac Imaging* 2017; 32: 137–150.
13 Rovere G, Meduri A, Savino G, *et al.* Practical instructions for using drugs in CT and MR cardiac imaging. *Radiol Med* 2021; 126: 356–364.
14 Pugliese L, Ricci F, Sica G, *et al.* Non-contrast and contrast-enhanced cardiac computed tomography imaging in the diagnostic and prognostic evaluation of coronary artery disease. *Diagnostics (Basel)* 2023; 13: 2074.
15 Flohr T, Petersilka M, Henning A, *et al.* Photon-counting CT review. *Phys Med* 2020; 79: 126–136.
16 National Institute for Health and Care Excellence. Addendum to Clinical Guideline (CG95), Chest pain of recent onset: Assessment and diagnosis. 2016. www.nice.org.uk/guidance/GID-CGWAVE0774/documents/addendum
17 Qanadli SD, El Hajjam M, Vieillard-Baron A, *et al.* New CT index to quantify arterial obstruction in pulmonary embolism. *Am J Roentgenol* 2001; 176: 1415–1420.
18 Weidman EK, Plodkowski AJ, Halpenny DF, *et al.* Dual-energy CT angiography for detection of pulmonary emboli: incremental benefit of iodine maps. *Radiology* 2018; 289: 546–553.
19 Patel BV, Arachchillage DJ, Ridge CA, *et al.* Pulmonary angiopathy in severe COVID-19: physiologic, imaging, and hematologic observations. *Am J Respir Crit Care Med* 2020; 202: 690–699.
20 Leitman EM, McDermott S. Pulmonary arteries: imaging of pulmonary embolism and beyond. *Cardiovasc Diagn Ther* 2019; 9: Suppl. 1, S37–S58.
21 Breunig M, Hanson A, Huckabee M. Learning curves for point-of-care ultrasound image acquisition for novice learners in a longitudinal curriculum. *Ultrasound J* 2023; 15: 31.
22 Ron E, Alattar Z, Hoebee S, *et al.* Current trends in the use of ultrasound over chest X-ray to identify pneumothoraces in ICU, trauma, and ARDS patients. *J Intensive Care Med* 2022; 37: 5–11.
23 Sistani SS, Parooie F. Diagnostic performance of ultrasonography in patients with pneumonia: an updated comparative systematic review and meta-analysis. *J Diagnostic Med Sonogr* 2021; 37: 371–381.
24 Bandi V, Lunn W, Ernst A, *et al.* Ultrasound *vs*. CT in detecting chest wall invasion by tumor: a prospective study. *Chest* 2008; 133: 881–886.
25 Volpicelli G, Elbarbary M, Blaivas M, *et al.* International evidence-based recommendations for point-of-care lung ultrasound. *Intensive Care Med* 2012; 38: 577–591.
26 Gargani L, Doveri M, D'Errico L, *et al.* Ultrasound lung comets in systemic sclerosis: a chest sonography hallmark of pulmonary interstitial fibrosis. *Rheumatology* 2009; 48: 1382–1387.
27 Lichtenstein DA, Mezière GA. Relevance of lung ultrasound in the diagnosis of acute respiratory failure: the BLUE protocol. *Chest* 2008; 134: 117–125.
28 Bouhemad B, Zhang M, Lu Q, *et al.* Clinical review: bedside lung ultrasound in critical care practice. *Crit Care* 2007; 11: 205.
29 Gargani L, Volpicelli G. How I do it: lung ultrasound. *Cardiovasc Ultrasound* 2014; 12: 25.

30 Miller A. Practical approach to lung ultrasound. *BJA Education* 2016; 16: 39–45.
31 Bhoil R, Ahluwalia A, Chopra R, *et al.* Signs and lines in lung ultrasound. *J Ultrason* 2021; 21: e225–e233.
32 Laursen CB, Clive A, Hallifax R, *et al.* European Respiratory Society statement on thoracic ultrasound. *Eur Respir J* 2021; 57: 2001519.
33 Roberts ME, Rahman NM, Maskell NA, *et al.* British Thoracic Society guideline for pleural disease. *Thorax* 2023; 78: Suppl. 3, s1–s42.
34 Park B, Park J, Shin KM, *et al.* Ultrasound-guided lung biopsy for small (⩽2 cm) subpleural lung lesions: comparison of diagnostic yield and safety with larger lesions. *J Thorac Dis* 2023; 15: 2485–2496.
35 Chen W, Zhang Y, Tang J, *et al.* Correlations between contrast-enhanced ultrasound and microvessel density in non-small cell lung cancer: a prospective study. *Front Oncol* 2023; 13: 1086251.
36 Quarato CMI, Feragalli B, Lacedonia D, *et al.* Contrast-enhanced ultrasound in distinguishing between malignant and benign peripheral pulmonary consolidations: the debated utility of the contrast enhancement arrival time. *Diagnostics (Basel)* 2023; 13: 666.
37 Mallow C, Isakow W. Risk factors for loss of lung sliding in a medical intensive care population with acute respiratory failure. *J Bronchology Interv Pulmonol* 2019; 26: 102–107.
38 Sartori S, Postorivo S, Vece FD, *et al.* Contrast-enhanced ultrasonography in peripheral lung consolidations: what's its actual role? *World J Radiol* 2013; 5: 372–380.
39 Sigrist RMS, Liau J, Kaffas AE, *et al.* Ultrasound elastography: review of techniques and clinical applications. *Theranostics* 2017; 7: 1303–1329.
40 Tárnoki D, Tárnoki Á, Karlinger K, *et al.* Az Interstitialis Tüdőbetegségek Képalkotása Multidiszciplináris Kitekintéssel [Imaging of Interstitial Lung Diseases with a Multidisciplinary Perspective]. Budapest, Medicina Könyvkiadó, 2020.
41 Radiopaedia. Fibrosing mediastinitis. Date last accessed: 1 December 2023. https://radiopaedia.org/articles/fibrosing-mediastinitis
42 Solomon SB, Ridge CA. CT-guided intervention in the thorax. *In:* Schoepf UJ, Meinel FG, eds. Multidetector-Row CT of the Thorax. 2nd Edn. Cham, Springer, 2016; pp. 545–564.
43 Coley SM, Crapanzano JP, Saqi A. FNA, core biopsy, or both for the diagnosis of lung carcinoma: obtaining sufficient tissue for a specific diagnosis and molecular testing. *Cancer Cytopathol* 2015; 123: 318–326.
44 Kuban JD, Tam AL, Huang SY, *et al.* The effect of needle gauge on the risk of pneumothorax and chest tube placement after percutaneous computed tomographic (CT)-guided lung biopsy. *Cardiovasc Intervent Radiol* 2015; 38: 1595–1602.
45 Ilie M, Hofman V, Dietel M, *et al.* Assessment of the PD-L1 status by immunohistochemistry: challenges and perspectives for therapeutic strategies in lung cancer patients. *Virchows Arch* 2016; 468: 511–525.
46 Vansteenkiste J, Crinò L, Dooms C, *et al.* 2nd ESMO Consensus Conference on Lung Cancer: early-stage non-small-cell lung cancer consensus on diagnosis, treatment and follow-up. *Ann Oncol* 2014; 25: 1462–1474.
47 Donington J, Ferguson M, Mazzone P, *et al.* American College of Chest Physicians and Society of Thoracic Surgeons consensus statement for evaluation and management for high-risk patients with stage I non-small cell lung cancer. *Chest* 2012; 142: 1620–1635.
48 Quirk MT, Pomykala KL, Suh RD. Current readings: percutaneous ablation for pulmonary metastatic disease. *Semin Thorac Cardiovasc Surg* 2014; 26: 239–248.
49 Pereira PL, Masala S. Standards of practice: guidelines for thermal ablation of primary and secondary lung tumors. *Cardiovasc Intervent Radiol* 2012; 35: 247–254.
50 Ridge CA, McErlean AM, Ginsberg MS. Epidemiology of lung cancer. *Semin Intervent Radiol* 2013; 30: 93–98.
51 Rose SC, Dupuy DE, Gervais DA, *et al.* Research reporting standards for percutaneous thermal ablation of lung neoplasms. *J Vasc Interv Radiol* 2009; 20: Suppl. 7, S474–S485.
52 Petre EN, Solomon SB, Sofocleous CT. The role of percutaneous image-guided ablation for lung tumors. *Radiol Med* 2014; 119: 541–548.
53 Cheng M, Fay M, Steinke K. Percutaneous CT-guided thermal ablation as salvage therapy for recurrent non-small cell lung cancer after external beam radiotherapy: a retrospective study. *Int J Hyperthermia* 2016; 32: 316–323.
54 Ridge CA, Solomon SB, Thornton RH. Thermal ablation of stage I non-small cell lung carcinoma. *Semin Intervent Radiol* 2014; 31: 118–124.
55 Ambrogi MC, Fanucchi O, Cioni R, *et al.* Long-term results of radiofrequency ablation treatment of stage I non-small cell lung cancer: a prospective intention-to-treat study. *J Thorac Oncol* 2011; 6: 2044–2051.
56 Dupuy DE, Fernando HC, Hillman S, *et al.* Radiofrequency ablation of stage IA non-small cell lung cancer in medically inoperable patients: results from the American College of Surgeons Oncology Group Z4033 (Alliance) trial. *Cancer* 2015; 121: 3491–3498.
57 Zemlyak A, Moore WH, Bilfinger TV. Comparison of survival after sublobar resections and ablative therapies for stage I non-small cell lung cancer. *J Am Coll Surg* 2010; 211: 68–72.

58 Pennathur A, Luketich JD, Abbas G, *et al.* Radiofrequency ablation for the treatment of stage I non-small cell lung cancer in high-risk patients. *J Thorac Cardiovasc Surg* 2007; 134: 857–864.
59 Hiraki T, Gobara H, Iishi T, *et al.* Percutaneous radiofrequency ablation for clinical stage I non-small cell lung cancer: results in 20 nonsurgical candidates. *J Thorac Cardiovasc Surg* 2007; 134: 1306–1312.
60 Hsie M, Morbidini-Gaffney S, Kohman LJ, *et al.* Definitive treatment of poor-risk patients with stage I lung cancer: a single institution experience. *J Thorac Oncol* 2009; 4: 69–73.
61 Lanuti M, Sharma A, Digumarthy SR, *et al.* Radiofrequency ablation for treatment of medically inoperable stage I non-small cell lung cancer. *J Thorac Cardiovasc Surg* 2009; 137: 160–166.
62 Hiraki T, Gobara H, Mimura H, *et al.* Radiofrequency ablation of lung cancer at Okayama University Hospital: a review of 10 years of experience. *Acta Med Okayama* 2011; 65: 287–297.
63 Liu B, Liu L, Hu M, *et al.* Percutaneous radiofrequency ablation for medically inoperable patients with clinical stage I non-small cell lung cancer. *Thorac Cancer* 2015; 6: 327–333.
64 Simon CJ, Dupuy DE, DiPetrillo TA, *et al.* Pulmonary radiofrequency ablation: long-term safety and efficacy in 153 patients. *Radiology* 2007; 243: 268–275.
65 Yang X, Ye X, Zheng A, *et al.* Percutaneous microwave ablation of stage I medically inoperable non-small cell lung cancer: clinical evaluation of 47 cases. *J Surg Oncol* 2014; 110: 758–763.
66 Han X, Yang X, Ye X, *et al.* Computed tomography-guided percutaneous microwave ablation of patients 75 years of age and older with early-stage nonsmall cell lung cancer. *Indian J Cancer* 2015; 52: Suppl. 2, e56–e60.
67 Palussiere J, Lagarde P, Aupérin A, *et al.* Percutaneous lung thermal ablation of non-surgical clinical N0 non-small cell lung cancer: results of eight years' experience in 87 patients from two centers. *Cardiovasc Intervent Radiol* 2015; 38: 160–166.
68 Zheng A, Ye X, Yang X, *et al.* Local efficacy and survival after microwave ablation of lung tumors: a retrospective study in 183 patients. *J Vasc Interv Radiol* 2016; 27: 1806–1814.
69 Zhong L, Sun S, Shi J, *et al.* Clinical analysis on 113 patients with lung cancer treated by percutaneous CT-guided microwave ablation. *J Thorac Dis* 2017; 9: 590–597.
70 Narsule CK, Sridhar P, Nair D, *et al.* Percutaneous thermal ablation for stage IA non-small cell lung cancer: long-term follow-up. *J Thorac Dis* 2017; 9: 4039–4045.
71 de Baère T, Palussière J, Aupérin A, *et al.* Midterm local efficacy and survival after radiofrequency ablation of lung tumors with minimum follow-up of 1 year: prospective evaluation. *Radiology* 2006; 240: 587–596.
72 Kwan SW, Mortell KE, Talenfeld AD, *et al.* Thermal ablation matches sublobar resection outcomes in older patients with early-stage non-small cell lung cancer. *J Vasc Interv Radiol* 2014; 25: 1–9.e1.
73 Vogl TJ, Eckert R, Naguib NN, *et al.* Thermal ablation of colorectal lung metastases: retrospective comparison among laser-induced thermotherapy, radiofrequency ablation, and microwave ablation. *AJR Am J Roentgenol* 2016; 207: 1340–1349.
74 Cheng G, Shi L, Qiang W, *et al.* The safety and efficacy of microwave ablation for the treatment of CRC pulmonary metastases. *Int J Hyperthermia* 2018; 34: 486–491.
75 Ferguson CD, Luis CR, Steinke K. Safety and efficacy of microwave ablation for medically inoperable colorectal pulmonary metastases: single-centre experience. *J Med Imaging Radiat Oncol* 2017; 61: 243–249.
76 Li L, Wu K, Lai H, *et al.* Clinical application of CT-guided percutaneous microwave ablation for the treatment of lung metastasis from colorectal cancer. *Gastroenterol Res Pract* 2017; 2017: 9621585.
77 Kurilova I, Gonzalez-Aguirre A, Beets-Tan RG, *et al.* Microwave ablation in the management of colorectal cancer pulmonary metastases. *Cardiovasc Intervent Radiol* 2018; 41: 1530–1544.
78 Tan C, Fisher OM, Huang L, *et al.* Comparison of microwave and radiofrequency ablation in the treatment of pulmonary metastasis of colorectal cancer. *Anticancer Res* 2022; 42: 4563–4571.
79 Reisenauer JS, Eiken PW, Callstrom MR, *et al.* A prospective trial of CT-guided percutaneous microwave ablation for lung tumors. *J Thorac Dis* 2022; 14: 939–951.
80 Carrafiello G, Mangini M, Fontana F, *et al.* Complications of microwave and radiofrequency lung ablation: personal experience and review of the literature. *Radiol Med* 2012; 117: 201–213.
81 Palussière J, Canella M, Cornelis F, *et al.* Retrospective review of thoracic neural damage during lung ablation – what the interventional radiologist needs to know about neural thoracic anatomy. *Cardiovasc Intervent Radiol* 2013; 36: 1602–1613.
82 Ricardi U, Badellino S, Filippi AR. Stereotactic radiotherapy for early stage non-small cell lung cancer. *Radiat Oncol J* 2015; 33: 57–65.
83 Kothary N, Dieterich S, Louie JD, *et al.* A primer on image-guided radiation therapy for the interventional radiologist. *J Vasc Interv Radiol* 2009; 20: 859–862.
84 Yoshida Y, Inoh S, Murakawa T, *et al.* Preoperative localization of small peripheral pulmonary nodules by percutaneous marking under computed tomography guidance. *Interact Cardiovasc Thorac Surg* 2011; 13: 25–28.
85 Liu L, Zhang LJ, Chen B, *et al.* Novel CT-guided coil localization of peripheral pulmonary nodules prior to video-assisted thoracoscopic surgery: a pilot study. *Acta Radiol* 2014; 55: 699–706.

86 Nakashima S, Watanabe A, Obama T, *et al.* Need for preoperative computed tomography-guided localization in video-assisted thoracoscopic surgery pulmonary resections of metastatic pulmonary nodules. *Ann Thorac Surg* 2010; 89: 212–218.
87 Imura M, Yamazaki K, Shirato H, *et al.* Insertion and fixation of fiducial markers for setup and tracking of lung tumors in radiotherapy. *Int J Radiat Oncol Biol Phys* 2005; 63: 1442–1447.
88 Tremblay A, Michaud G. Single-center experience with 250 tunnelled pleural catheter insertions for malignant pleural effusion. *Chest* 2006; 129: 362–368.
89 Putnam JB Jr, Light RW, Rodriguez RM, *et al.* A randomized comparison of indwelling pleural catheter and doxycycline pleurodesis in the management of malignant pleural effusions. *Cancer* 1999; 86: 1992–1999.
90 Almeida J, Leal C, Figueiredo L. Evaluation of the bronchial arteries: normal findings, hypertrophy and embolization in patients with hemoptysis. *Insights Imaging* 2020; 11: 70.
91 Panda A, Bhalla AS, Goyal A. Bronchial artery embolization in hemoptysis: a systematic review. *Diagn Interv Radiol* 2017; 23: 307–317.
92 Omachi N, Ishikawa H, Hara M, *et al.* The impact of bronchial artery embolisation on the quality of life of patients with haemoptysis: a prospective observational study. *Eur Radiol* 2021; 31: 5351–5360.
93 Kaufman CS, Kwan SW. Bronchial artery embolization. *Semin Intervent Radiol* 2022; 39: 210–217.
94 Kucher N, Boekstegers P, Müller OJ, *et al.* Randomized, controlled trial of ultrasound-assisted catheter-directed thrombolysis for acute intermediate-risk pulmonary embolism. *Circulation* 2014; 129: 479–486.
95 Piazza G, Hohlfelder B, Jaff MR, *et al.* A prospective, single-arm, multicenter trial of ultrasound-facilitated, catheter-directed, low-dose fibrinolysis for acute massive and submassive pulmonary embolism: the SEATTLE II study. *JACC Cardiovasc Interv* 2015; 8: 1382–1392.
96 Sista AK, Horowitz JM, Tapson VF, *et al.* Indigo aspiration system for treatment of pulmonary embolism: results of the EXTRACT-PE trial. *JACC Cardiovasc Interv* 2021; 14: 319–329.
97 Tu T, Toma C, Tapson VF *et al.* A prospective, single-arm, multicenter trial of catheter-directed mechanical thrombectomy for intermediate-risk acute pulmonary embolism: the FLARE study. *JACC Cardiovasc Interv* 2019; 12: 859–869.
98 Silver MJ, Gibson CM, Giri J, *et al.* Outcomes in high-risk pulmonary embolism patients undergoing FlowTriever mechanical thrombectomy or other contemporary therapies: results from the FLAME study. *Circ Cardiovasc Interv* 2023; 16: e013406.
99 Toma C, Jaber WA, Weinberg MD, *et al.* Acute outcomes for the full US cohort of the FLASH mechanical thrombectomy registry in pulmonary embolism. *EuroIntervention* 2023; 18: 1201–1212.
100 Bajc M, Schümichen C, Grüning T, *et al.* EANM guideline for ventilation/perfusion single-photon emission computed tomography (SPECT) for diagnosis of pulmonary embolism and beyond. *Eur J Nucl Med Mol Imaging* 2019; 46: 2429–2451.
101 Chen DL, Kinahan PE. Multimodality molecular imaging of the lung. *Clin Transl Imaging* 2014; 2: 391–401.
102 Kusmirek JE, Magnusson JD, Perlman SB. Current applications for nuclear medicine imaging in pulmonary disease. *Curr Pulmonol Rep* 2020; 9: 82–95.
103 Falk GL, Beattie J, Ing A, *et al.* Scintigraphy in laryngopharyngeal and gastroesophageal reflux disease: a definitive diagnostic test? *World J Gastroenterol* 2015; 21: 3619–3627.
104 Zhu J, Pan F, Cai H, *et al.* Positron emission tomography imaging of lung cancer: an overview of alternative positron emission tomography tracers beyond F18 fluorodeoxyglucose. *Front Med (Lausanne)* 2022; 9: 945602.
105 Groheux D, Quere G, Blanc E, *et al.* FDG PET-CT for solitary pulmonary nodule and lung cancer: literature review. *Diagn Interv Imaging* 2016; 97: 1003–1017.
106 Frood R, McDermott G, Scarsbrook A. Respiratory-gated PET/CT for pulmonary lesion characterisation – promises and problems. *Br J Radiol* 2018; 91: 20170640.
107 Ganeshalingam S, Koh DM. Nodal staging. *Cancer Imaging* 2009; 9: 104–111.
108 Chao F, Zhang H. PET/CT in the staging of the non-small-cell lung cancer. *J Biomed Biotechnol* 2012; 2012: 783739.
109 Fisseler-Eckhoff A, Demes M. Neuroendocrine tumors of the lung. *Cancers (Basel)* 2012; 4: 777–798.
110 Lococo F, Cesario A, Paci M, *et al.* PET/CT assessment of neuroendocrine tumors of the lung with special emphasis on bronchial carcinoids. *Tumour Biol* 2014; 35: 8369–8377.
111 Fiebrich HB, de Jong JR, Kema IP, *et al.* Total ^{18}F-dopa PET tumour uptake reflects metabolic endocrine tumour activity in patients with a carcinoid tumour. *Eur J Nucl Med Mol Imaging* 2011; 38: 1854–1861.
112 Huang Y, Fan J, Li Y, *et al.* Imaging of tumor hypoxia with radionuclide-labeled tracers for PET. *Front Oncol* 2021; 11: 731503.
113 Niu G, Chen X. PET imaging of angiogenesis. *PET Clin* 2009; 4: 17–38.
114 Chandekar KR, Prashanth A, Vinjamuri S, *et al.* FAPI PET/CT imaging – an updated review. *Diagnostics (Basel)* 2023; 13: 2018.
115 Lillington J, Brusaferri L, Kläser K, *et al.* PET/MRI attenuation estimation in the lung: a review of past, present, and potential techniques. *Med Phys* 2020; 47: 790–811.

116 Furtado FS, Hesami M, McDermott S, *et al.* The synergistic effect of PET/MRI in whole-body oncologic imaging: an expert review. *Clin Transl Imaging* 2023; 11: 351–364.

117 Kwon HW, Becker AK, Goo JM, *et al.* FDG whole-body PET/MRI in oncology: a systematic review. *Nucl Med Mol Imaging* 2017; 51: 22–31.

118 Spick C, Herrmann K, Czernin J. ^{18}F-FDG PET/CT and PET/MRI perform equally well in cancer: evidence from studies on more than 2,300 patients. *J Nucl Med* 2016; 57: 420–430.

119 Wang ML, Zhang H, Yu HJ, *et al.* An initial study on the comparison of diagnostic performance of ^{18}F-FDG PET/MR and ^{18}F-FDG PET/CT for thoracic staging of non-small cell lung cancer: focus on pleural invasion. *Rev Esp Med Nucl Imagen Mol (Engl Ed)* 2023; 42: 16–23.

120 Yeung JC, Donahoe LL, Hinzpeter R, *et al.* Thoracic imaging. *In:* Catalano OA, ed. Clinical PET/MRI. London, Academic Press, 2023; pp. 179–198.

121 Filippov A, Bonjoc KC, Chea J, *et al.* Role of theranostics in thoracic oncology. *J Thorac Dis* 2020; 12: 5140–5146.

122 Zhu T, Hsu JC, Guo J, *et al.* Radionuclide-based theranostics – a promising strategy for lung cancer. *Eur J Nucl Med Mol Imaging* 2023; 50: 2353–2374.

123 Jamar F, Buscombe J, Chiti A, *et al.* EANM/SNMMI guideline for ^{18}F-FDG use in inflammation and infection. *J Nucl Med* 2013; 54: 647–658.

124 Capitanio S, Nordin AJ, Noraini AR, *et al.* PET/CT in nononcological lung diseases: current applications and future perspectives. *Eur Respir Rev* 2016; 25: 247–258.

125 Vass L, Fisk M, Lee S, *et al.* Advances in PET to assess pulmonary inflammation: a systematic review. *Eur J Radiol* 2020; 130: 109182.

126 Rolle AM, Hasenberg M, Thornton CR, *et al.* ImmunoPET/MR imaging allows specific detection of *Aspergillus fumigatus* lung infection *in vivo*. *Proc Natl Acad Sci USA* 2016; 113: E1026–E1033.

Suggested answers

1. a. Irreversible bleeding diathesis is an absolute contraindication to CT-guided lung biopsy. Biopsy provides a means to obtain not only a diagnosis of primary or metastatic cancer, but also to pursue molecular testing to provide treatment specific to the tumour subtype.
2. b. Pneumothorax in approximately 20% of patients can occur after lung tumour ablation; this is treated with chest drain insertion. There is typically no decline in lung function after ablation. Death is rare after CT-guided lung tumour ablation. The current reported local recurrence rate after MWA of lung metastases is approximately 10%.
3. b. Talc pleurodesis and tunnelled pleural catheter placement are appropriate treatment options for malignant pleural effusion; however, if a pleural effusion accumulates rapidly after drainage, pleurodesis is not likely to be successful.
4. a. CDT is often associated with a desired decline in the RV/LV ratio as a marker of improving RV failure. Death, pneumonia and access-related haematoma are not common events after CDT.
5. c.
6. a.
7. b and d.
8. d.
9. b.